

1 **Appendix: Supplementary material for**  
2 **“Habitat fragmentation and species diversity in**  
3 **competitive communities”**

4 November 19, 2019

5 Joel Rybicki · joel.rybicki@ist.ac.at

6 Nerea Abrego · nerea.abrego@helsinki.fi

7 Otso Ovaskainen · otso.ovaskainen@helsinki.fi

8 **Contents**

|    |   |           |
|----|---|-----------|
| 9  | <b>A Prior work on metacommunity models</b>                                 | <b>4</b>  |
| 10 | <b>B Description of the simulation model</b>                                | <b>5</b>  |
| 11 | B.1 Details of the spatially-explicit community model . . . . .             | 5         |
| 12 | B.1.1 Model structure . . . . .   | 5         |
| 13 | B.1.2 Resource patch dynamics . . . . .                                     | 6         |
| 14 | B.1.3 Species dynamics . . . . .  | 6         |
| 15 | B.1.4 Comparison to a deterministic, non-spatial model . . . . .            | 7         |
| 16 | B.1.5 Dispersal . . . . .   | 8         |
| 17 | B.1.6 Habitat fragmentation . . . . .                                       | 9         |
| 18 | B.1.7 Large-scale environmental variation in habitat types . . . . .        | 9         |
| 19 | B.1.8 Simulation of the individual-based model . . . . .                    | 11        |
| 20 | B.2 Meanfield approximation of species dynamics . . . . .                   | 11        |
| 21 | B.3 Displacement of resource-deprived individuals . . . . .                 | 13        |
| 22 | <b>C Sensitivity of the simulation model and additional experiments</b>     | <b>14</b> |
| 23 | C.1 Convergence to the stationary state . . . . .                           | 14        |
| 24 | C.2 A neutral model with no variation in resource types . . . . .           | 14        |
| 25 | C.3 Sensitivity to the number of species . . . . .                          | 14        |
| 26 | C.4 Sensitivity to the size of the landscape . . . . .                      | 15        |
| 27 | C.5 Testing the sample area effect with larger sampling sites . . . . .     | 15        |
| 28 | C.6 An alternative parameterisation of the individual-based model . . . . . | 16        |

29 **List of Figures**

30 S1 Examples of fragmented landscapes . . . . . 18

31 S2 Comparison of the spatial stochastic model against the deterministic meanfield model 19

32 S3 The average density of resource-satiated individuals vs. time . . . . . 20

33 S4 SLOSS analysis, neutral community, 128 species . . . . . 21

34 S5 SFAR analysis, neutral community, 128 species . . . . . 22

35 S6 Species richness vs. fragmentation, neutral community, 128 species . . . . . 23

36 S7 SLOSS analysis, neutral community, 64 species . . . . . 24

37 S8 SFAR analysis, neutral community, 64 species . . . . . 25

38 S9 Species richness vs. fragmentation, neutral community, 64 species . . . . . 26

39 S10 Inferring local scale for HAH, neutral community, 64 species,  $\tau = 1$  . . . . . 27

40 S11 Inferring local scale for HAH, neutral community, 64 species,  $\tau = 2$  . . . . . 28

41 S12 SLOSS analysis, environmental gradient, 64 species . . . . . 29

42 S13 SFAR analysis, environmental gradient, 64 species . . . . . 30

43 S14 Species richness vs. fragmentation, environmental gradient, 64 species . . . . . 31

44 S15 Inferring local scale for HAH, environmental gradient, 64 species,  $\tau = 1$  . . . . . 32

45 S16 Inferring local scale for HAH, environmental gradient, 64 species,  $\tau = 2$  . . . . . 33

46 S17 SLOSS analysis, neutral community, 32 species . . . . . 34

47 S18 SFAR analysis, neutral community, 32 species . . . . . 35

48 S19 Species richness vs. fragmentation, neutral community, 32 species . . . . . 36

49 S20 Inferring local scale for HAH, neutral community, 32 species,  $\tau = 1$  . . . . . 37

50 S21 Inferring local scale for HAH, neutral community, 32 species,  $\tau = 2$  . . . . . 38

51 S22 SLOSS analysis, environmental gradient, 32 species . . . . . 39

52 S23 SFAR analysis, environmental gradient, 32 species . . . . . 40

53 S24 Species richness vs. fragmentation, environmental gradient, 32 species . . . . . 41

54 S25 Inferring local scale for HAH, environmental gradient, 32 species,  $\tau = 1$  . . . . . 42

55 S26 Inferring local scale for HAH, environmental gradient, 32 species,  $\tau = 2$  . . . . . 43

56 S27 SLOSS analysis in a small  $25 \times 25$  landscape . . . . . 44

57 S28 SFAR analysis in a small  $25 \times 25$  landscape . . . . . 45

58 S29 Species richness vs. fragmentation in a small  $25 \times 25$  landscape . . . . . 46

59 S30 SLOSS analysis in a small  $25 \times 25$  landscape with an environmental gradient . . . . . 47

|    |   |    |
|----|---|----|
| 60 | S31 SFAR analysis in a small $25 \times 25$ landscape with an environmental gradient . . . . .    | 48 |
| 61 | S32 Species richness vs. fragmentation in a small $25 \times 25$ landscape with an environmental- |    |
| 62 | gradient . . . . .  | 49 |
| 63 | S33 Inferring local scale for HAH, 128 species, environmental gradient, $\tau = 2$ . . . . .      | 50 |
| 64 | S34 SLOSS analysis, alternative neutral parameterisation . . . . .                                | 51 |
| 65 | S35 SFAR analysis, alternative neutral parameterisation . . . . .                                 | 52 |
| 66 | S36 Species richness vs. fragmentation, alternative neutral parameterisation . . . . .            | 53 |
| 67 | S37 SLOSS analysis, alternative parameterisation, environmental gradient . . . . .                | 54 |
| 68 | S38 SFAR analysis, alternative parameterisation, environmental gradient . . . . .                 | 55 |
| 69 | S39 Species richness vs. fragmentation, alternative parameterisation, environmental gradient      | 56 |

70 **List of Tables**

|    |  |    |
|----|--|----|
| 71 | S1 Parameters of the community model and their default values . . . . .                  | 10 |
| 72 | S2 Results for the HAH test in landscapes with sampling site radius $\tau = 2$ . . . . . | 15 |
| 73 | S3 Results for the HAH test in neutral communities of 128 species, sampling site radius  |    |
| 74 | $\tau = 1$ . . . . .   | 15 |
| 75 | S4 Results for the HAH test in neutral communities of 128 species, sampling site radius  |    |
| 76 | $\tau = 2$ . . . . .   | 16 |

## 77 **A Prior work on metacommunity models**

78 We focus on species dynamics at the landscape level in fragmented environments, that is, metacom-  
79 munity dynamics. While a metapopulation is a collection of populations (of a single species) that  
80 reside in discrete patches connected by dispersal, the metacommunity concept is its multispecies  
81 analogue (Hanski, 1999): patches are inhabited by several (possibly interacting) species and the  
82 metacommunity dynamics are governed by various coexistence processes (Leibold et al., 2004).  
83 Typically, theoretical studies on metacommunities have generalised patch-based metapopulation  
84 models into multispecies models with discrete patches in both spatially-implicit (Tilman et al., 1994,  
85 Loreau et al., 2003, Mouquet and Loreau, 2003, Allouche and Kadmon, 2009, Wang and Loreau,  
86 2016) and spatially-explicit models (Solé et al., 2004, Rybicki and Hanski, 2013, Matias et al., 2014,  
87 Thompson et al., 2014, Fournier et al., 2016, Thompson et al., 2017). The interspecies interactions  
88 are typically competitive (e.g. competition on space or a shared limiting resource) (Tilman et al.,  
89 1994, Loreau et al., 2003, Mouquet and Loreau, 2003, Solé et al., 2004, Wang and Loreau, 2016,  
90 Matias et al., 2014, Thompson et al., 2014, Fournier et al., 2016, Thompson et al., 2017), but also  
91 mutualistic (e.g. plant-pollinator systems) (Klausmeier, 2001, Prakash and de Roos, 2004, Fortuna  
92 and Bascompte, 2006) and trophic interactions (Pillai et al., 2010) have been considered.

93 A relatively large proportion of the theoretical work on metacommunities has focused on un-  
94 derstanding how e.g. coexistence mechanisms and dispersal maintain species diversity and stabil-  
95 ity (Lehman and Tilman, 2000, Loreau et al., 2003, Mouquet and Loreau, 2003, Gravel et al., 2006,  
96 Logue et al., 2011, Haegeman and Loreau, 2014, Wang and Loreau, 2016, Gravel et al., 2016). While  
97 less common, models have also been used to investigate how landscape structure, habitat loss and  
98 fragmentation influence species richness in metacommunities (Tilman et al., 1997, Solé et al., 2004,  
99 Prakash and de Roos, 2004, Rybicki and Hanski, 2013, Matias et al., 2014, Thompson et al., 2014,  
100 2017, Xu et al., 2018).

101 As usual, these models make various assumptions for the sake of tractability: some completely  
102 ignore species interactions and rely on species-sorting mechanisms (Rybicki and Hanski, 2013),  
103 limit to only pairs of interacting species (Klausmeier, 2001), ignore spatial heterogeneity, assume  
104 patch-based metapopulation dynamics (Tilman et al., 1997, Prakash and de Roos, 2004, Rybicki  
105 and Hanski, 2013, Matias et al., 2014) or lack demographic and/or environmental stochasticity by  
106 employing deterministic, continuous-valued dynamics (Thompson et al., 2014).

## 107 B Description of the simulation model

### 108 B.1 Details of the spatially-explicit community model

109 We first define the model dynamics in a pristine landscape without habitat loss. After this, we  
110 discuss ways how to include habitat loss and fragmentation into our model. For brevity, we describe  
111 the model in the context of a single species consuming a single resource type, but the model is  
112 straightforward to generalise to multiple species and resource types.

#### 113 B.1.1 Model structure

114 Formally, our model is a spatiotemporal point process, or in the mathematical terminology, a Markov  
115 evolution in the space of locally finite configurations (see e.g. [Ovaskainen et al., 2014](#)). The state of a  
116 model at any given time is given by the spatial location of each individual of each type. The dynamics  
117 of the model can be described by listing all events that can take place and the rates at which these  
118 events occur. These rates can depend on the current spatial configuration of all individuals (e.g.  
119 individuals can only consume resources that are within their proximity). The proximity-dependence  
120 is described via kernels, that is, functions that tell at which rate two particles at locations  $x = (x_1, x_2)$   
121 and  $y = (y_1, y_2)$  react depending on their Euclidean distance  $\text{dist}(x, y)$ . A kernel  $K(x, y) = r \cdot f(x, y)$   
122 is defined in terms of a total rate parameter  $r$  and a density function  $f$ , which describes how the  
123 total rate  $r$  is distributed across the space.

124 We use two types of kernels. A *tophat* kernel  $K$  with length scale  $\ell$  and total rate  $r$  is defined as

$$K(x, y) = \begin{cases} \frac{r}{2\pi\ell^2} & \text{if } \text{dist}(x, y) \leq \ell, \\ 0 & \text{otherwise.} \end{cases}$$

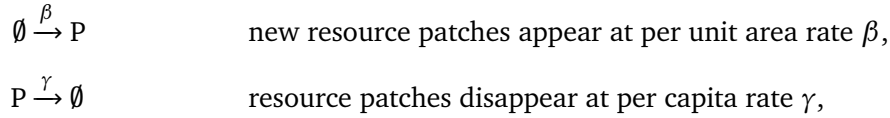
125 A *Gaussian* kernel  $K$  with length scale  $\ell$  and total rate  $r$  is given by

$$K(x, y) = A(r) \cdot \exp\left(-\frac{\text{dist}(x, y)^2}{2\ell^2}\right),$$

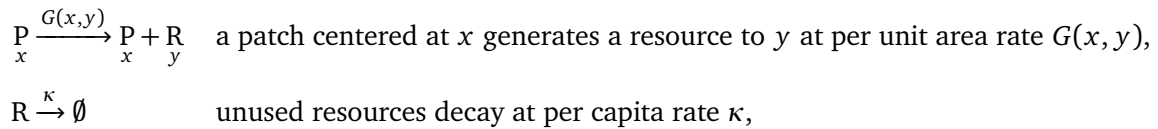
126 where  $A(r) = r/(2\pi\ell^2)$  is a normalisation constant such that  $K$  integrates to the value  $r$ . In the  
127 following, we write  $\ell(K)$  and  $r(K)$  to denote the length scale and total rate of kernel  $K$  of either type.

128 **B.1.2 Resource patch dynamics**

129 To obtain spatiotemporal variation in resource production rate, we assume that the resource patches  
 130 follow birth-death dynamics independent of the species. The resource patch birth-death dynamics  
 131 are described by the following processes



132 where  $\emptyset$  denotes “no particle” (i.e. birth of resource patches does not depend on any entity and  
 133 the death of a patch simply removes the patch but not the resource units it has produced). We  
 134 assume that the resource patches are circular (but may overlap) and that a resource patch located at  
 135  $x$  produces abiotic resource units to its surroundings according to the tophat resource generation  
 136 kernel  $G$ . Resource units that are left unconsumed by the species decay and disappear with constant  
 137 rate  $\kappa$ . Thus, we have the following processes:

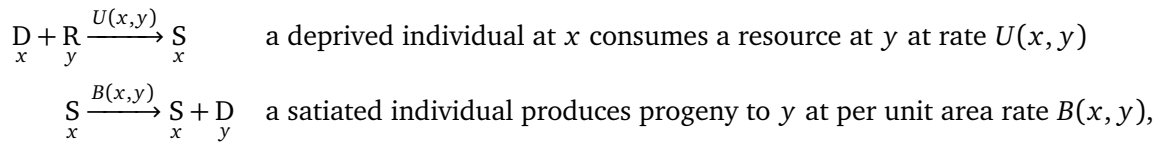


138 where in the first reaction, the location of a new particle is randomly sampled according to the  
 139 density function  $f$  of the kernel  $G(x, y) = r \cdot f(x, y)$ . Note that we can control the spatiotemporal  
 140 properties of the landscape’s habitat quality by varying the per unit area density  $\rho = \beta/\gamma$  of habitat  
 141 patches, the patch turnover rate  $\gamma$ , the resource production rate  $r = r(G)$ , and the radius  $\ell(G)$  of the  
 142 patches. First panel of Fig. S1 depicts an example snapshot of the resulting habitat structure.

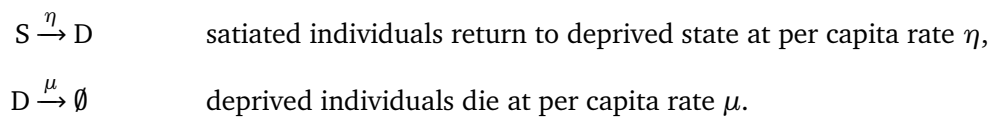
143 **B.1.3 Species dynamics**

144 The species follow birth-death dynamics and individuals have two states. Newborn individuals start  
 145 out in the *resource-deprived* state, and upon consuming a resource unit, they become *resource-satiated*;  
 146 for brevity, we refer to individuals in these states as deprived (D) and satiated (S), respectively. The

147 satiated individuals produce new individuals into their surroundings:



148 where  $U$  is a tophat resource utilisation kernel,  $B$  is a Gaussian birth kernel, and the satiated  
 149 individuals give birth to new individuals at total per capita rate of  $r(B)$  and the locations of the  
 150 new deprived individuals are sampled according to the density function of  $B$ . Eventually, satiated  
 151 individuals become resource-deprived, and if they do not consume resources, they die:



152 In addition to birth by resource-satiated individuals, we assume that there is a small background rate  
 153 of influx immigration into the focal landscape:



#### 154 B.1.4 Comparison to a deterministic, non-spatial model

155 As a brief digression, let us check that the above resource-consumer model makes sense by considering  
 156 the deterministic dynamics in a non-spatial setting, which is easy to analyse (see Appendix B.2).  
 157 There exists a unique positive equilibrium of satiated individuals if all rates are positive. In case  
 158  $\alpha = 0$ , that is, when there is no immigration of individuals outside the focal landscape, the species  
 159 goes extinct if the total resource production rate is not sufficiently high. More precisely, there exists  
 160 an extinction threshold of

$$\frac{G\beta}{\kappa\gamma} > \frac{\eta\mu}{BU},$$

161 where  $G, B, U$  correspond to the total rates (i.e. integrals) of the respective kernels. Thus, the  
 162 meanfield approximation exhibits the expected dynamics of resource-consumer models: without  
 163 immigration, the resource equilibrium level determines whether the consumer can persist in the  
 164 system. Now let us return to the stochastic, spatially-explicit and individual-based model with  
 165 heterogeneous habitat structure.

166 **B.1.5 Dispersal**

167 We consider two modes of dispersal for the species:

- 168 • *passive* (one-shot) dispersal, where an individual does not move during its life time,
- 169 • *active* dispersal, where resource-deprived individuals move to find suitable habitat.

170 For passive dispersal, individuals only move when they are born according to the birth kernel  $B$   
 171 centered around their progenitor. In active dispersal, we include an additional movement process for  
 172 resource-deprived individuals:

$$D_x \xrightarrow{M(x,y)} D_y \quad \text{resource-deprived individuals jump from } x \text{ to } y \text{ at per unit area rate } M(x, y).$$

173 The idea is that in the active mode of dispersal, resource-deprived individuals can make additional  
 174 movements to move from a location lacking resources to a new location with resources. Once an  
 175 individual finds resources and consumes them, it becomes resource-satiated and stops moving.

176 We control the length of dispersal with the scale parameter  $\delta$  and the mode of dispersal with  
 177 an integer parameter  $k > 0$ . We set length scales of the Gaussian birth and movement kernels to  
 178  $\ell(B) = \ell(M) = \delta/\sqrt{k}$  and set the movement rate to  $r(M) = (k-1)\mu$ . Passive dispersal corresponds  
 179 to case  $k = 1$ , as no movement after birth occurs. In active dispersal, we have  $k > 1$ . Thus, species  
 180 with passive dispersal are sessile, whereas species with active dispersal are not.

181 Note that regardless of the value  $k$ , the new location of an actively dispersing resource-deprived  
 182 individual during its lifetime has the same mean and variance as a passive disperser *assuming the*  
 183 *individual does not become satiated at any point in its lifetime*. If an individual remains resource-  
 184 deprived its entire lifetime, then the number of dispersal steps  $s$  is a random variable with an  
 185 expectation of  $r(M)/\mu$  (see Appendix B.3). Hence, as an individual always make a single movement  
 186 step at birth, the total displacement is a random variable  $x = (x_1, x_2)$  that satisfies

$$x_i | s = \sum_{j=0}^s x_{ij},$$

187 where  $i \in \{1, 2\}$  and  $x_{ij} \sim \mathcal{N}(0, \delta^2/k)$  are independent Gaussian variables. It follows that  $x_i$  has the  
 188 same mean 0 and variance  $\delta^2$  in both the active and passive dispersal modes (see Appendix B.3).



### 189 B.1.6 Habitat fragmentation

190 Above we have described the model in a pristine landscape with no habitat loss or fragmentation;  
191 while the habitat quality (resource production rate) can have patchy structure, the spatiotemporal  
192 dynamics of the resource patches guarantee that every location of the landscape has statistically the  
193 same properties over time.

194 We conduct our simulations in a finite focal landscape of size  $V \times V$ , which is assumed to be part  
195 of a larger landscape that has statistically similar structure everywhere. To avoid boundary effects, we  
196 assume it to be a two-dimensional torus  $\mathcal{L} \subseteq \mathbb{R}^2$ . In order to model habitat loss and fragmentation,  
197 we assume that the focal landscape  $\mathcal{L}$  is partitioned into  $N$  disjoint (non-overlapping) circular *habitat*  
198 *fragments*, where the habitat fragment  $i$  is centered at location  $x_i$  and consists of all points within  
199 radius  $r_i$ . The *matrix*  $\mathcal{M}$  then consists of the points that are not part of any habitat fragment. We  
200 emphasise that the notions of *habitat fragment* and *resource patch* (an entity that produces abiotic  
201 resource units into its surroundings) refer to distinct concepts in our model.

202 We generate *fragmented* landscapes where the patch sizes follow a log-normal distribution so that  
203 there are patches of various sizes. Given the total habitat cover  $0 < C < 1$  and number of fragments  
204  $N > 0$ , we sample the relative area of each fragment  $A_i \sim \exp \mathcal{N}(\mu, \sigma^2)$  with parameters  $\mu = 1/2$   
205 and  $\sigma = 1$  for every fragment  $i \in \{1, \dots, N\}$  and normalise the areas so that  $\sum A_i = C \cdot V^2$ .

206 The fragments are placed onto the landscape in a decreasing order in area and both coordinates  
207 of the fragment  $i$  are sampled uniformly at random from the interval  $[0, V]$ , where  $V$  is the parameter  
208 controlling the size of the focal landscape. The coordinates of fragment  $i$  are resampled until there  
209 is no overlap with any fragment  $j < i$  to ensure that all fragments are disjoint. Fig. S1 illustrates  
210 examples of fragmented landscapes for different values of  $C$  and  $N$ . For the special case  $C = 1$ , we  
211 assume that the entire landscape is covered by a single fragment.

### 212 B.1.7 Large-scale environmental variation in habitat types

213 In the main text, we consider a variant of the model with large-scale environmental variation in  
214 habitat types. Here, the species are divided into four groups, each of which is specialised to a certain  
215 type of a resource. The resource distributions follow different environmental gradients, but the  
216 overall resource production rate is the same for each resource type throughout the landscape (in a  
217 non-fragmented setting). Thus, while the species rely on different resource types, the species are  
218 equivalent in the sense of having the same expected fitness: all species have the same parameters

Table S1: Parameters of the community model and their default values

| Process                                     | Name     | Value / Rate ( $r$ ) | Length scale ( $\ell$ ) |
|---|----------|----------------------|-------------------------|
| Patch birth rate (per unit area)            | $\beta$  | 0.01                 | –                       |
| Patch turnover/death rate (per capita)      | $\gamma$ | 0.1                  | –                       |
| Resource decay rate (per capita)            | $\kappa$ | 0.1                  | –                       |
| Resource production kernel (tophat)         | $G$      | 4                    | 2                       |
| Resource utilisation kernel (tophat)        | $U$      | 1                    | 0.5                     |
| Resource deprivation rate (per capita)      | $\eta$   | 0.1                  | –                       |
| Mortality rate (per capita)                 | $\mu$    | 1                    | –                       |
| Background immigration rate (per unit area) | $\alpha$ | 0.001                | –                       |
| Dispersal scale parameter                   | $\delta$ | 1, 3, 10             | –                       |
| Mode of dispersal parameter                 | $k$      | 4                    | –                       |
| Birth kernel (Gaussian)                     | $B$      | 1                    | $\delta/\sqrt{k}$       |
| Movement kernel (Gaussian)                  | $M$      | $(k-1)\mu$           | $\delta/\sqrt{k}$       |

219 (Table S1) and the landscape produces all types of resource at the same rate. Later below, we also  
 220 consider a *completely neutral* model (Hubbell, 2001), where all species are identical and consume  
 221 exactly the same resource type.

222 **Generating large-scale environmental variation.** We assumed that there were four distinct re-  
 223 source patch types each producing a distinct resource type. Each species  $i$  was then specialised to  
 224 consume only resources of type  $i \bmod 4 + 1$ . To produce environmental gradients for the habitat  
 225 types, the location of a new resource patch of type  $j \in \{1, 2, 3, 4\}$  was sampled according to the  
 226 density function  $g_j(x, y)$  on  $[0, 1]^2$ , where

$$g_1(x, y) = 1 + \sin(2\pi x)$$

$$g_2(x, y) = 1 + \sin(2\pi x + \pi)$$

$$g_3(x, y) = 1 + \sin(2\pi y)$$

$$g_4(x, y) = 1 + \sin(2\pi y + \pi).$$

227 The sampled coordinates were then scaled to the domain size of  $V \times V$  of the focal landscape. In  
 228 this setting, the landscapes are heterogeneous also in terms of habitat types in addition to habitat  
 229 quality. We conducted the experiments described in the main text also for the nine scenarios under  
 230 (1) specialist communities in landscapes with large-scale environmental gradients in habitat types  
 231 and (2) completely neutral communities with no variation in habitat types.

232 **B.1.8 Simulation of the individual-based model**

233 To simulate the individual-based model, we use the Gibson–Bruck next reaction method (Gibson  
 234 and Bruck, 2000), a Gillespie-style simulation algorithm (Gillespie, 1976). The algorithm produces  
 235 exact stochastic trajectories of the stochastic individual-based model. The algorithm is adapted to the  
 236 spatial setting similarly as done by Cornell et al. (2019). The source code for the simulation software  
 237 used in this work is available online (Rybicki et al., 2019).

238 **B.2 Meanfield approximation of species dynamics**

239 Let us examine the single-species dynamics in a non-spatial setting. If we assume that the system is  
 240 well-mixed and let the length scale  $\ell \rightarrow \infty$  for each kernel, then the deterministic meanfield model  
 241 can be written as

$$\begin{aligned}\frac{dP}{dt} &= \beta - \gamma P \\ \frac{dR}{dt} &= GP - \kappa R - UDR \\ \frac{dS}{dt} &= UDR - \eta S \\ \frac{dD}{dt} &= \alpha + (\eta + B)S - \mu D - UDR,\end{aligned}$$

242 where the capital letter  $X$  denotes the integral  $r(X)$  of the kernel  $X$ ,  $\alpha$  is non-negative and all other  
 243 parameters are positive. The two non-trivial equilibria are

$$\begin{aligned}\hat{P} &= \frac{\beta}{\gamma} \\ \hat{R} &= [a + b(c + d) - \xi] \cdot \frac{1}{2BU\kappa\gamma} \\ \hat{S} &= [a - b(c + d) + \xi] \cdot \frac{1}{2BU\eta\gamma} \\ \hat{D} &= [a + b(d - c) + \xi] \cdot \frac{1}{2U\eta\mu\gamma},\end{aligned}$$

244 where we abbreviate

$$a = \beta B U G$$

$$b = \gamma \eta$$

$$c = \kappa \mu$$

$$d = \alpha U$$

$$\xi = \pm \sqrt{(a + b(c + d))^2 - 4abc}.$$

245 Since we have  $a, b, c > 0$  and  $d \geq 0$ , this yields that  $\xi$  is real, as

$$(a + b(c + d))^2 - 4abc = (a - bc)^2 + bd(2a + (b(2c + d))) > 0.$$

246 Therefore, a unique positive equilibrium  $\hat{S} > 0$  of satiated individuals exists when

$$a - b(c + d) \pm \sqrt{(a + b(c + d))^2 - 4abc} > 0.$$

247 If the third term has a negative sign, the condition cannot be satisfied. However, if the third term has  
248 a positive sign, then the condition is always satisfied if all parameters  $a, b, c, d > 0$  are positive. In  
249 the case that  $\alpha = 0$ , that is, there is no immigration of individuals from outside the focal landscape,  
250 we have  $d = 0$  and a positive equilibrium exists only if  $a > bc$  holds. Rewriting this condition gives

$$\frac{G\beta}{\kappa\gamma} > \frac{\eta\mu}{BU},$$

251 where the left-hand side corresponds to the resource density of the habitat in the absence of the  
252 species. Thus, without outside immigration, the species cannot persist if the total amount and/or  
253 quality of habitat is not sufficiently high. In other words, we obtain an extinction threshold for the  
254 deterministic, non-spatial single-species model in the absence of outside immigration.

255 **Comparison between the spatially-explicit stochastic model and the meanfield model.** As the  
256 size parameter of the domain  $V \rightarrow \infty$  goes to infinity, the stochastic model approaches the meanfield  
257 model in the limit of large-scale interactions (length scales  $\ell \rightarrow \infty$ ). This is illustrated by Fig. S2.

258 **B.3 Displacement of resource-deprived individuals**

259 **Expected number of jumps.** A resource-deprived individual will die at rate  $\mu$  and jumps at rate  
 260  $r = r(M)$ . Let  $s$  be the number of jumps a resource-deprived individual makes in its lifetime assuming  
 261 it never becomes satiated (excluding the initial jump at birth). The number of jumps during an  
 262 interval of length  $T$  is a random variable  $X|T \sim \text{Poisson}(\lambda)$  with  $\lambda = rT$ . The length of the interval  
 263  $T$  is an exponentially distributed random variable  $T \sim \text{Exp}(\mu)$ . Thus,

$$\begin{aligned} \Pr[s = k] &= \int_{t=0}^{\infty} \Pr[s = k|T = t] \cdot f(t; \mu) dt \\ &= \int_{t=0}^{\infty} e^{-rt} \frac{(rt)^k}{k!} \cdot f(t; \mu) dt \\ &= \int_{t=0}^{\infty} e^{-rt} \frac{(rt)^k}{k!} \cdot \mu e^{-\mu t} dt \\ &= \frac{\mu r^k}{(\mu + r)^{k+1}}, \end{aligned}$$

264 where  $f(t; \mu)$  is the probability density function of the exponential distribution. The expected number  
 265  $E[s]$  of jumps is

$$E[s] = \sum_{k=0}^{\infty} k \cdot \Pr[s = k] = \sum_{k=0}^{\infty} \frac{k \mu r^k}{(\mu + r)^{k+1}} = r/\mu.$$

266 **Total displacement.** The total displacement in coordinate  $i$  is a random variable

$$\sum_{j=0}^s x_{ij},$$

267 where  $x_{ij} \sim \mathcal{N}(0, \delta^2/k)$  are independent Gaussian random variables (recall that  $x_{i0}$  is the initial  
 268 displacement at birth). Since the expectation of  $x_{ij}$  is zero, the total displacement satisfies

$$E \left[ \sum_{j=0}^s x_{ij} \right] = (1 + E[s]) \cdot 0 = 0 \quad \text{and} \quad \text{Var} \left[ \sum_{j=1}^s x_{ij} \right] = (1 + E[s]) \cdot \delta^2/k = \delta^2,$$

269 as  $E[s] = r(M)/\mu = (k - 1)\mu/\mu = k - 1$ .

## 270 **C Sensitivity of the simulation model and additional experiments**

271 In this section, we provide additional experiments that show the model is robust to small changes to  
272 the assumptions and parameter values used. For example, we investigate the case of a completely  
273 neutral model (without environmental gradients in resource types), varying the number of species,  
274 and changing the size of the focal landscape. All variants provide qualitatively similar results. We  
275 start by showing that the simulation times are sufficient to reach a stationary state.

### 276 **C.1 Convergence to the stationary state**

277 All the simulation experiments were conducted with a simulation time  $T = 400$  time units. Fig. S3  
278 shows that on average the density of resource-satiated individuals quickly converges towards the  
279 stationary state well before 400 time units.

### 280 **C.2 A neutral model with no variation in resource types**

281 We considered a completely neutral variant of the model, where all the species compete on the same  
282 limiting resource. The patterns produced are similar to the ones produced by the non-neutral model  
283 with large-scale environmental variation in resource types. In the neutral setting, the all habitat  
284 areas produce the same type of resource. This yields that the effect of habitat loss on species richness  
285 is not as pronounced. For example, Fig. S6 does not show the downward slope of the unimodal curve  
286 in the second and third columns.

### 287 **C.3 Sensitivity to the number of species**

288 We repeated the main experiments underlying with 32 and 64 species (in contrast to the 128 species  
289 used in the main text). Irrespective of the number of species, the analyses yield qualitatively similar  
290 results (i.e. at high amount of total habitat fragmentation has positive effect, but at smaller amount  
291 of total habitat high levels of fragmentation tend have a negative effect on species richness):

- 292 • Results for a species pool of size  $S = 64$ :
  - 293 – neutral community: Fig. S7, Fig. S8, Fig. S9, Fig. S10, Fig. S11
  - 294 – environmental gradient: Fig. S12, Fig. S13 and Fig. S14, Fig. S15, Fig. S16.
- 295 • Results for a species pool of size  $S = 32$ :
  - 296 – neutral community: Fig. S17, Fig. S18 and Fig. S19,

#### 298 C.4 Sensitivity to the size of the landscape

299 The main experiments have been conducted in a landscape of size  $100 \times 100$ . We repeated the  
 300 experiments in smaller landscapes of size  $25 \times 25$ . Figures S27, S28, and S29 show that in these  
 301 smaller landscapes the SLOSS and SFAR analyses provide qualitatively same results, but the threshold  
 302 at which fragmentation effects appear is higher (as there is less absolute amount of habitat available).

#### 303 C.5 Testing the sample area effect with larger sampling sites

304 We repeated the analysis of the sample area effect using larger sampling sites (i.e. we increased the  
 305 radius  $\tau$  of sampling sites from 1 to 2). The results of the sample area effect analysis with a larger  
 306 sampling radius  $\tau = 2$  are given in Table S2 and Fig. S33.

|   | $\delta$ | $\beta_L (M_{L+F})$ | $\beta_F (M_{L+F})$ | $\beta_L (M_L)$ | $\beta_F (M_F)$ | AIC $M_{L+F}$ | AIC $M_L$ | AIC $M_F$ | AIC $M_{\text{null}}$ |
|---|----------|---------------------|---------------------|-----------------|-----------------|---------------|-----------|-----------|-----------------------|
| H | 1        | 0.31                | 0.01                | 0.34            | 0.09            | 0             | 0.73      | 206.61    | 631.67                |
| H | 3        | 0.35                | 0.03                | 0.41            | 0.16            | 0             | 21.96     | 567.51    | 2686.65               |
| H | 10       | 0.39                | 0.04                | 0.44            | 0.23            | 0             | 41.67     | 1376.99   | 5317.45               |
| P | 1        | 0.3                 | 0.02                | 0.35            | 0.09            | 0             | 5.51      | 185.89    | 654.47                |
| P | 3        | 0.34                | 0.05                | 0.44            | 0.16            | 0             | 56.92     | 477.59    | 2607.98               |
| P | 10       | 0.39                | 0.03                | 0.43            | 0.22            | 0             | 23.07     | 1601.34   | 5256.4                |
| A | 1        | 0.26                | 0.02                | 0.32            | 0.1             | 0             | 11.71     | 230.15    | 1024.24               |
| A | 3        | 0.28                | 0.01                | 0.29            | 0.13            | 0             | 0.39      | 583.72    | 2255.06               |
| A | 10       | 0.31                | -0.01               | 0.3             | 0.15            | 0             | 3.2       | 1719.37   | 3863.53               |

Table S2: Results for the HAH test in landscapes with sampling site radius  $\tau = 2$

|   | $\delta$ | $\beta_L (M_{L+F})$ | $\beta_F (M_{L+F})$ | $\beta_L (M_L)$ | $\beta_F (M_F)$ | AIC $M_{L+F}$ | AIC $M_L$ | AIC $M_F$ | AIC $M_{\text{null}}$ |
|---|----------|---------------------|---------------------|-----------------|-----------------|---------------|-----------|-----------|-----------------------|
| H | 1        | 0.22                | 0.03                | 0.28            | 0.1             | 0             | 11.11     | 99.28     | 550.35                |
| H | 3        | 0.21                | 0                   | 0.22            | 0.12            | 1.82          | 0         | 194.09    | 1072.13               |
| H | 10       | 0.2                 | 0                   | 0.2             | 0.13            | 2             | 0         | 306.7     | 1239.33               |
| P | 1        | 0.27                | 0.02                | 0.31            | 0.1             | 0             | 2.47      | 152.7     | 623.36                |
| P | 3        | 0.23                | 0                   | 0.23            | 0.11            | 1.99          | 0         | 189.4     | 911.92                |
| P | 10       | 0.18                | 0.03                | 0.21            | 0.14            | 0             | 8.82      | 197.53    | 1297.67               |
| A | 1        | 0.2                 | 0.02                | 0.23            | 0.1             | 0             | 2.61      | 108.59    | 627.28                |
| A | 3        | 0.14                | 0.02                | 0.17            | 0.09            | 0             | 3.17      | 87.91     | 673.77                |
| A | 10       | 0.11                | 0.02                | 0.13            | 0.09            | 0             | 3.78      | 141.05    | 638.52                |

Table S3: Results for the HAH test in neutral communities of 128 species, sampling site radius  $\tau = 1$

|   | $\delta$ | $\beta_L (M_{L+F})$ | $\beta_F (M_{L+F})$ | $\beta_L (M_L)$ | $\beta_F (M_F)$ | AIC $M_{L+F}$ | AIC $M_L$ | AIC $M_F$ | AIC $M_{\text{null}}$ |
|---|----------|---------------------|---------------------|-----------------|-----------------|---------------|-----------|-----------|-----------------------|
| H | 1        | 0.23                | 0.02                | 0.28            | 0.09            | 0             | 8.69      | 114.14    | 543.32                |
| H | 3        | 0.23                | 0                   | 0.23            | 0.11            | 1.7           | 0         | 297.11    | 1281.35               |
| H | 10       | 0.18                | 0.01                | 0.2             | 0.12            | 0             | 2         | 492.31    | 1803.83               |
| P | 1        | 0.26                | 0.01                | 0.28            | 0.08            | 0.41          | 0         | 152.08    | 525.55                |
| P | 3        | 0.23                | 0                   | 0.22            | 0.11            | 1.66          | 0         | 287.01    | 1236.04               |
| P | 10       | 0.18                | 0.02                | 0.21            | 0.12            | 0             | 5.79      | 316.61    | 1683.08               |
| A | 1        | 0.23                | 0.02                | 0.26            | 0.1             | 0             | 2.2       | 172.13    | 788.28                |
| A | 3        | 0.14                | 0.01                | 0.16            | 0.09            | 0             | 0.7       | 142.63    | 865.35                |
| A | 10       | 0.14                | -0.01               | 0.13            | 0.07            | 0             | 1.52      | 410.19    | 981.85                |

Table S4: Results for the HAH test in neutral communities of 128 species, sampling site radius  $\tau = 2$

### 307 C.6 An alternative parameterisation of the individual-based model

308 We also considered a parameterisation, where the species were more sensitive to resource availability,  
309 but in contrast had increased birth rates. Specifically, we changed the parameterisation as follows:

- 310 • resource units disappear faster when left unconsumed ( $\kappa$  was increased from 0.1 to 0.2),
- 311 • resource-satiated individuals become resource deprived faster ( $\eta$  increased from 0.2 to 0.5),
- 312 • resource-satiated individuals produce more propagules (birth rate  $B$  increased from 1 to 2).

313 Here, we used a species pool of  $S = 64$  species. We repeated the SFAR and SLOSS analyses for this  
314 parameterisation of the model with and without large-scale environmental gradients. We observed  
315 that the species communities became more sensitive to loss of habitat but also to fragmentation. The  
316 experiments are summarised in the following figures:

- 317 • SLOSS analysis *without* environmental gradient Fig. S34,
- 318 • SLOSS analysis *with* environmental gradient Fig. S37,
- 319 • SFAR analysis *without* environmental gradient Fig. S35 and Fig. S36,
- 320 • SFAR analysis *with* environmental gradient Fig. S38 and Fig. S39.

321 The SLOSS analyses show negative responses to fragmentation, particularly in the case with envi-  
322 ronmental gradients in habitat types (Fig. S34 and Fig. S37). We see that in both cases, the species  
323 become more sensitive to habitat loss, as the SFAR curves have steeper slopes (Fig. S35 and Fig. S38).  
324 Moreover, we see that species richness responds to fragmentation per se in a non-monotone way, but  
325 it is predominantly much less positive than in the prior parameterisation ((Fig. S36 and Fig. S39).  
326 We note that increasing fragmentation had little to no effect when the total amount of habitat was  
327 high (32% habitat cover), but in the alternative parameterisation with an environmental gradient



328 also these high levels of total habitat showed a non-monotone response to fragmentation (top lines  
329 in Fig. S39).

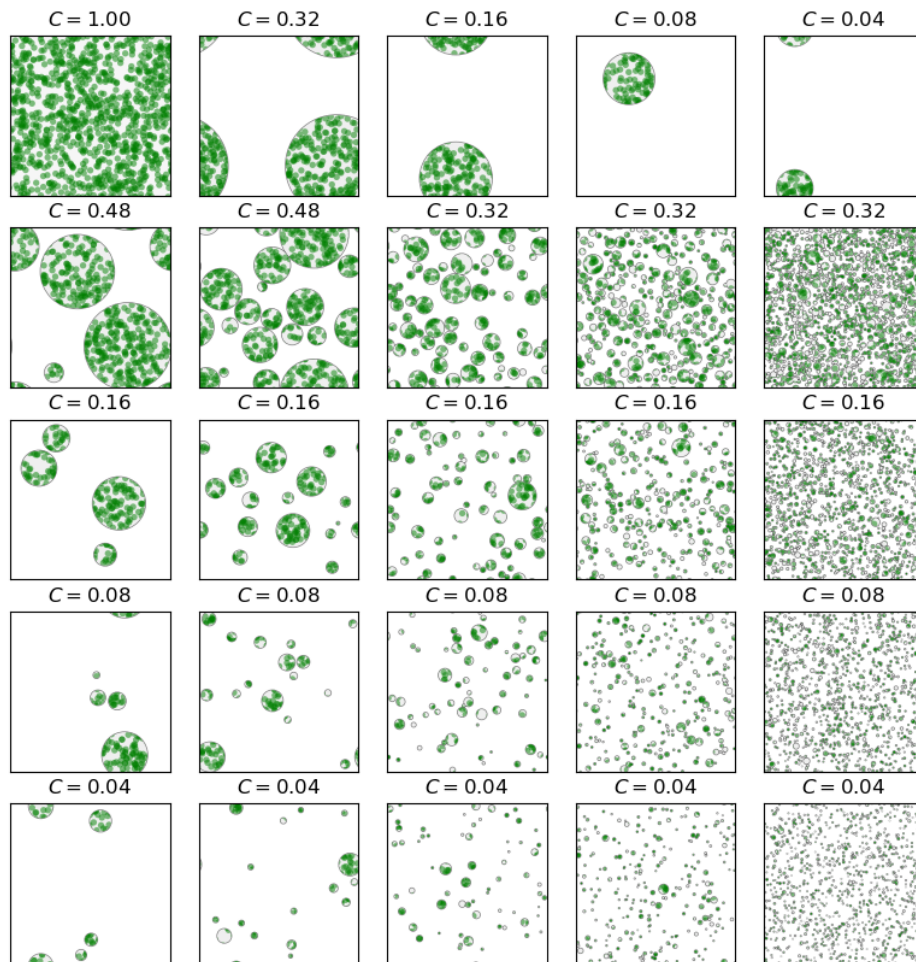


Figure S1: Examples of fragmented landscapes with varying levels of fragmentation and habitat cover. The landscape is a torus (i.e. periodic boundaries) of size  $100 \times 100$ . Green circles are resource patches, which may overlap to create higher resource production rates at some areas (darker green). The filled gray circles represent habitat fragments within which resource patches follow stochastic birth-death dynamics, and within these circles, the gray area represents habitat (currently) without resource patches. The white areas represent the matrix, that is, area which has zero resource production rate, as resource units cannot establish in the matrix. The habitat fragments do not overlap.

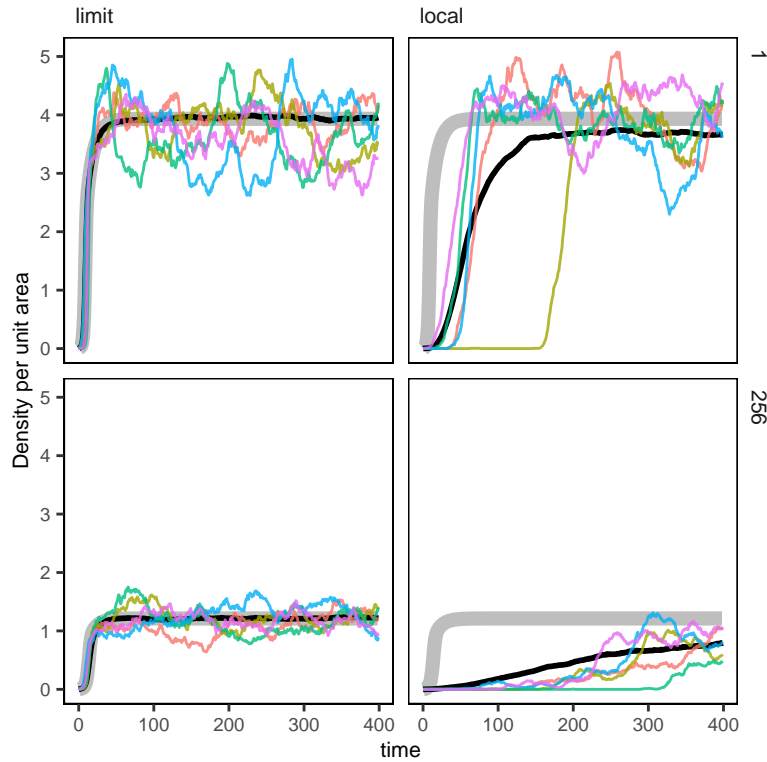


Figure S2: Comparison between the spatial stochastic model with a single species and the meanfield model. Here, to exaggarate the difference between the spatial and meanfield models, we have used a parameterization which differs from the parameterisation given in Table S1 as follows: the patch birth and turnover rates are  $\beta = 0.05$  and  $\gamma = 0.025$ , resource production rate is 2 (rate of  $G$ ), resource deprivation rate is  $\eta = 2$ , and birth rate is 1.5 (rate of  $B$ ). The spatial domain of the simulation is  $15 \times 15$ . The grey line is the equilibrium solution  $\hat{S}$  for the density of resource-satiated individuals, the coloured lines are example trajectories of the per unit area densities of resource satiated individuals in the stochastic area, and the black line gives the average density over 200 replicate trajectories. The column “limit“ considers simulations with length scales of all the kernels at  $V/2$ , whereas “local” has the length scales as before. The top row considers a scenario with completely intact landscape, whereas the bottom row considers a scenario with a landscape that has been fragmented to 256 habitat fragments that cover 16% of the simulation area.

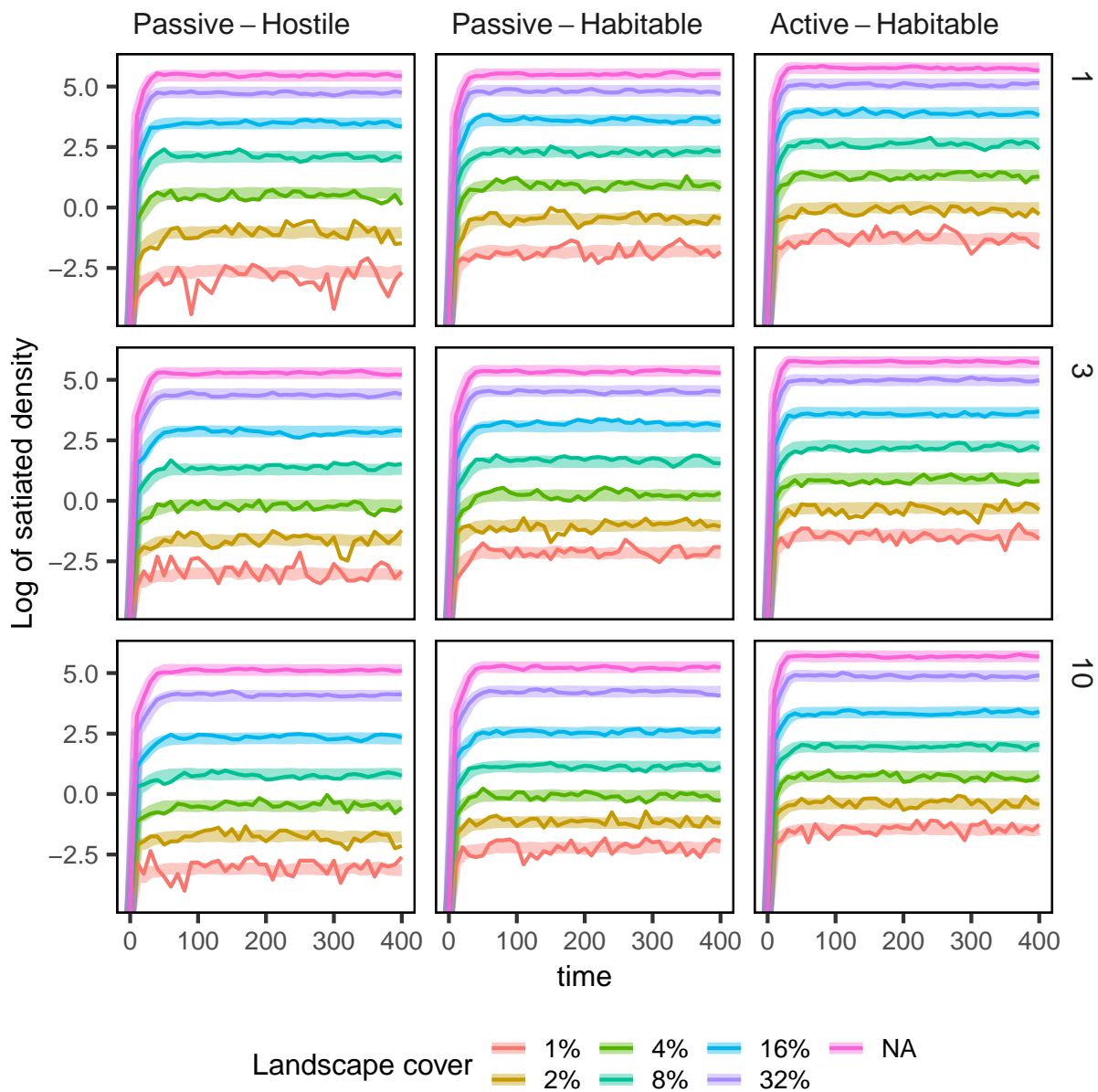


Figure S3: The average density of resource-satiated individuals over 100 replicate landscapes. The rows denote different values of the dispersal parameter  $\delta$  and each column considers a different dispersal/matrix scenario. In each panel, the thick lines give the average density of resource-satiated individuals across all simulation replicates as a function of time. The thin lines give the average density of resource-satiated individuals in a single replicate landscape. The figure shows the results for experiments where the focal landscapes have size  $100 \times 100$  and which have been fragmented into 256 parts.

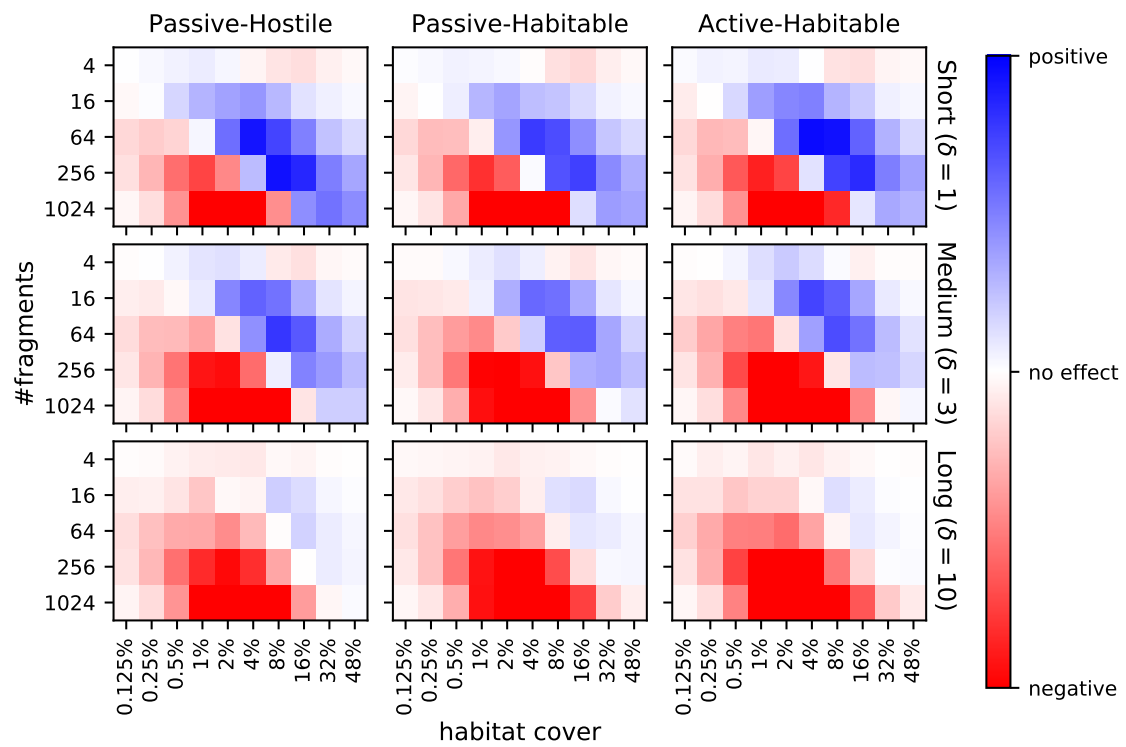


Figure S4: SLOSS analysis on a neutral community with 128 species.

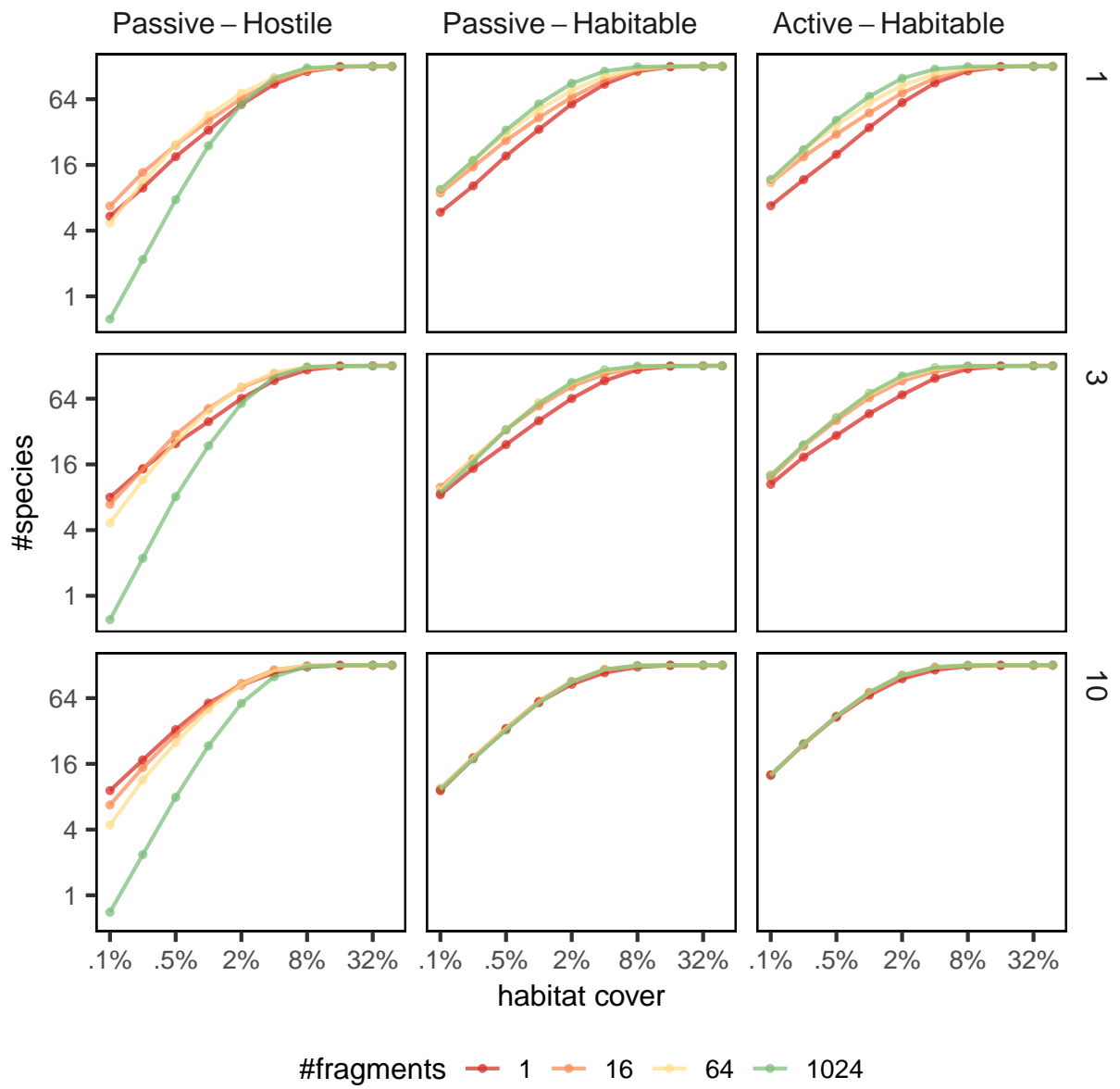


Figure S5: SFAR analysis on a neutral community with 128 species.

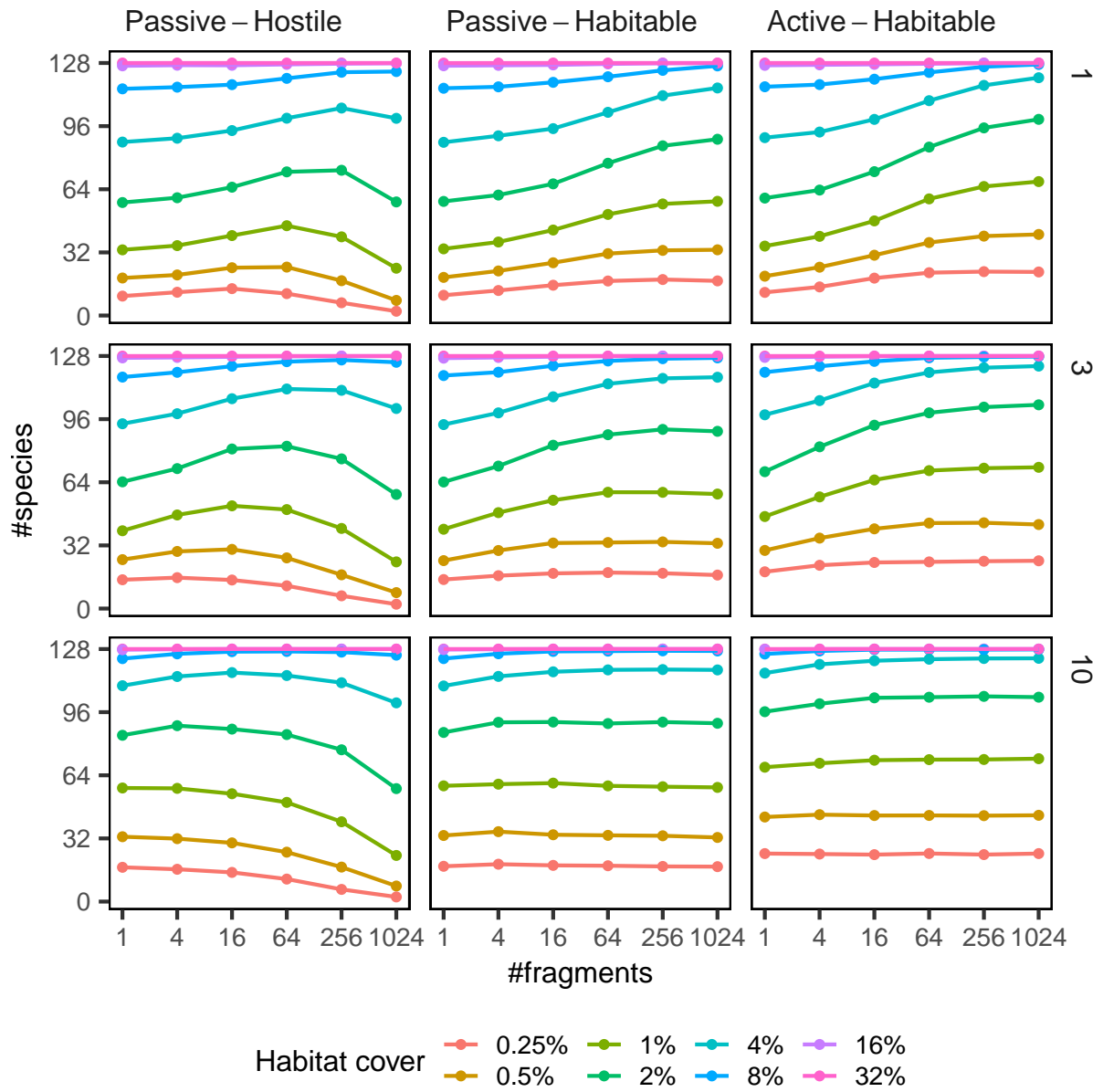


Figure S6: Species richness as a function of habitat fragmentation in a community with 128 species.

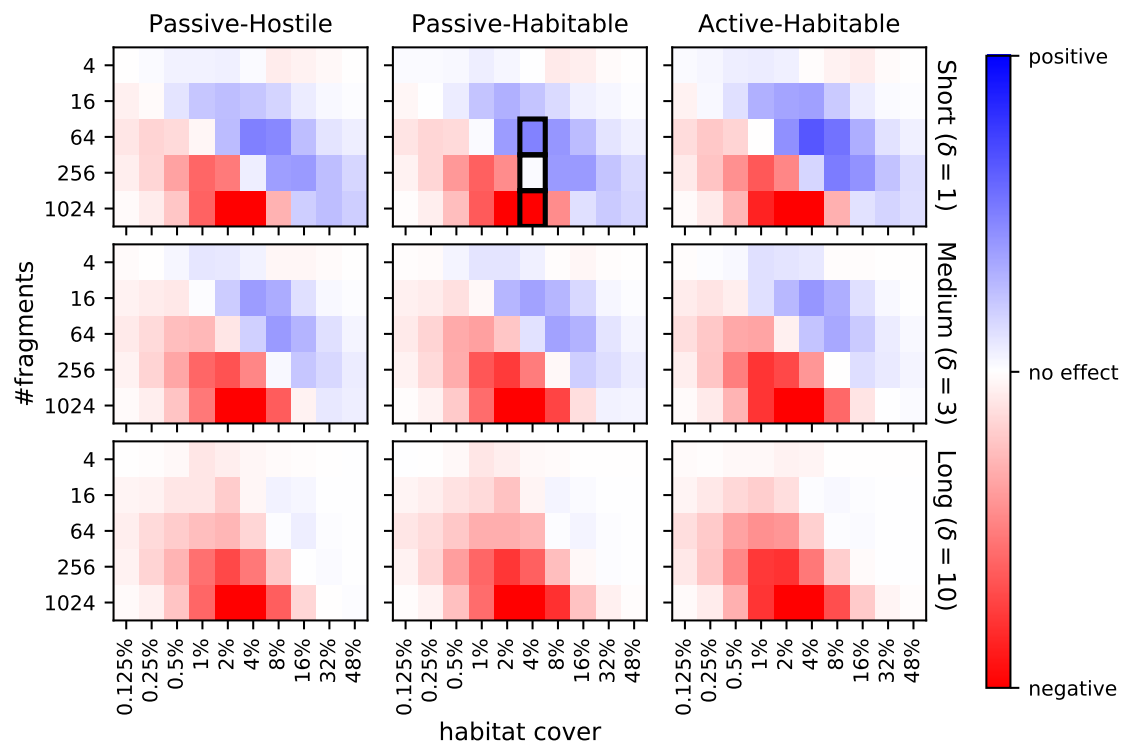


Figure S7: SLOSS analysis of the neutral community of 64 species in a  $100 \times 100$  landscape.



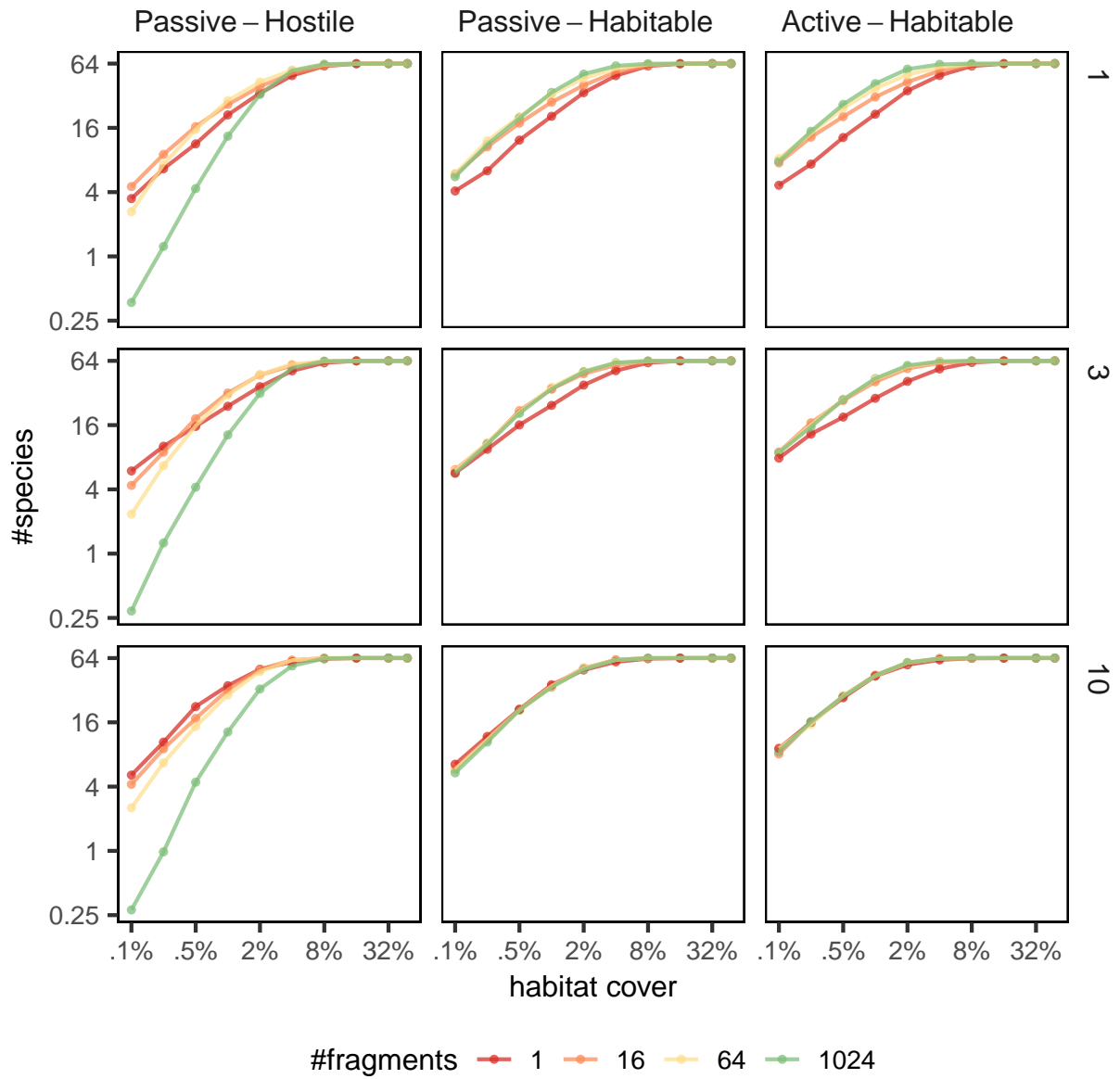


Figure S8: SFAR analysis on the neutral community of 64 species in a  $100 \times 100$  landscape.

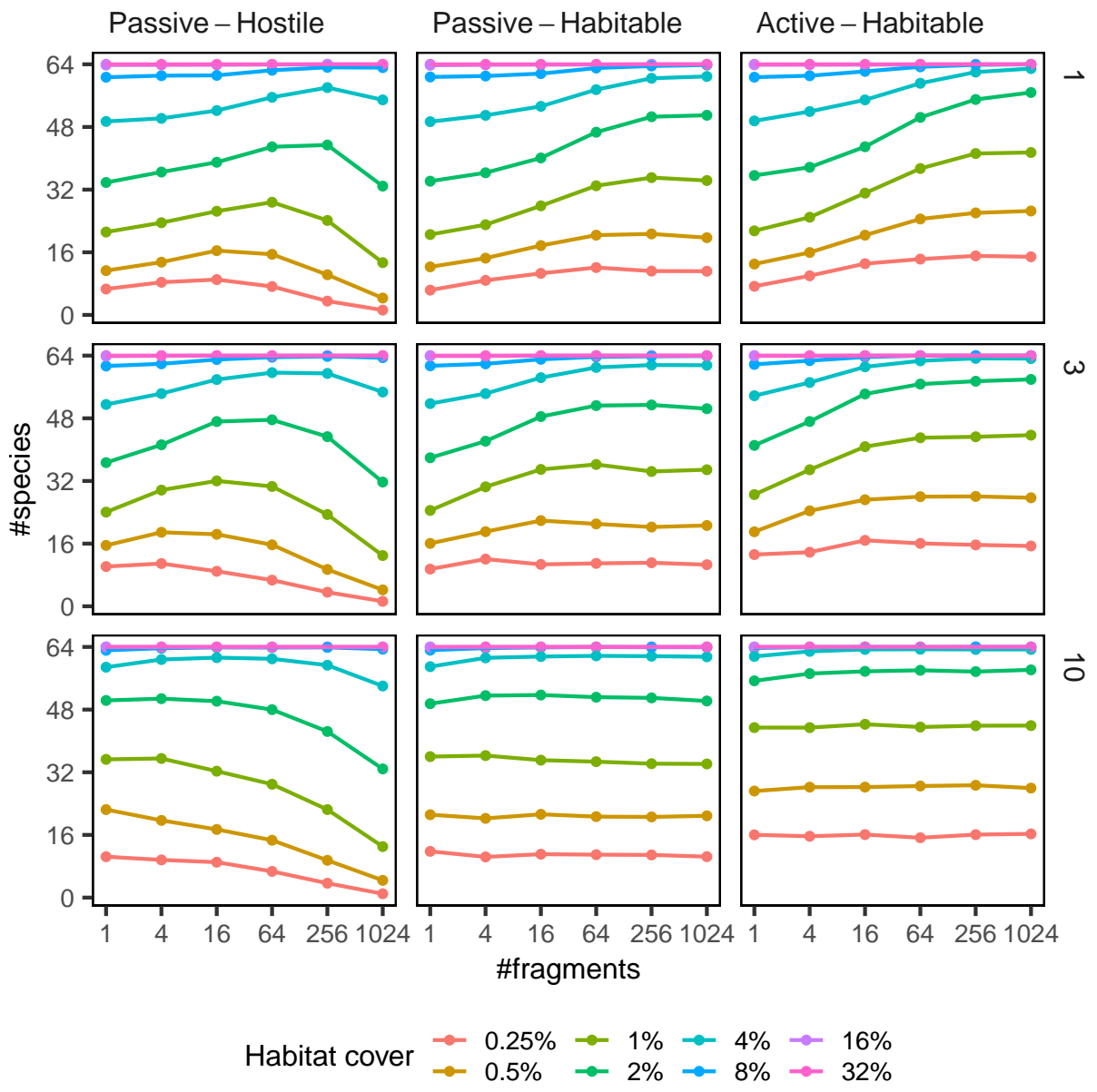


Figure S9: Species richness as a function of habitat fragmentation in a neutral community of 64 species in a  $100 \times 100$  landscape.

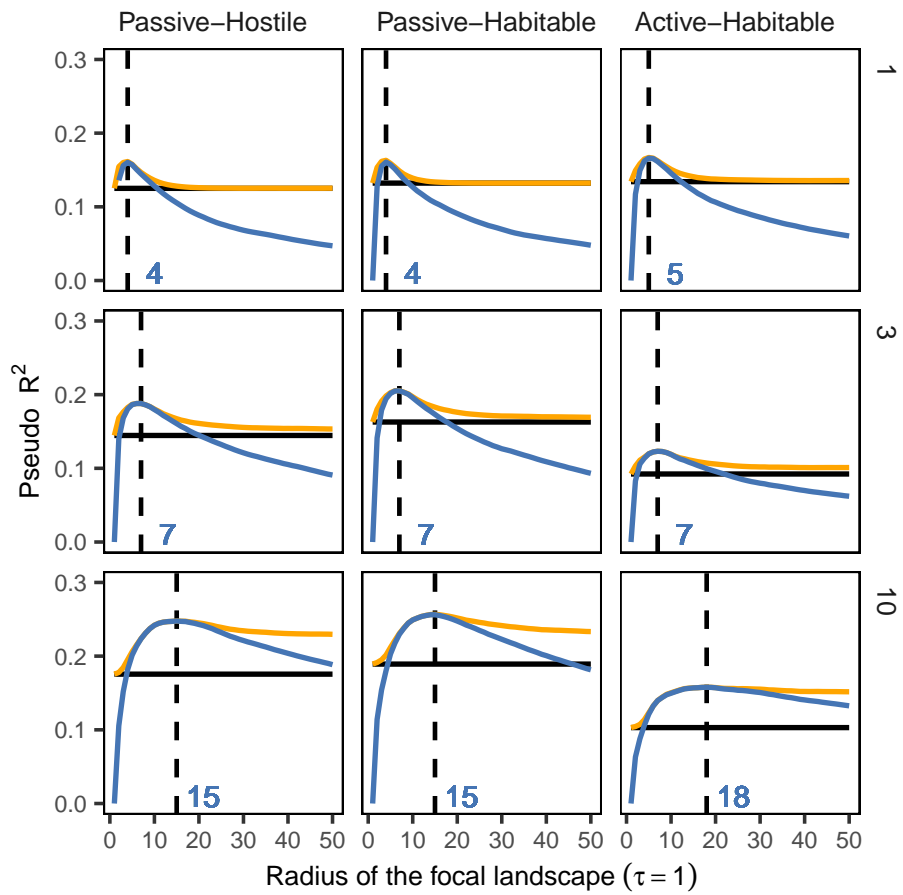


Figure S10: Inferring the appropriate scale of local landscape and testing the sample area effect on a neutral community of size 32. The radius of the sample site is  $\tau = 1$ .

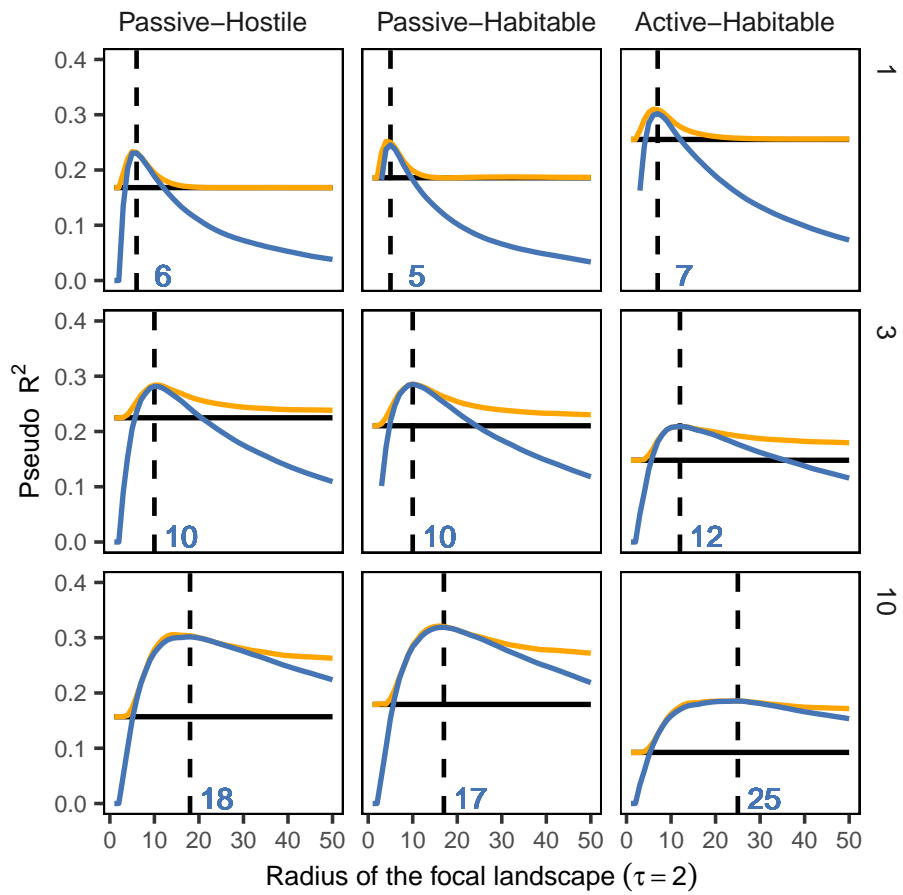


Figure S11: Inferring the appropriate scale of local landscape and testing the sample area effect on a neutral community of size 32. The radius of the sample site is  $\tau = 2$ .

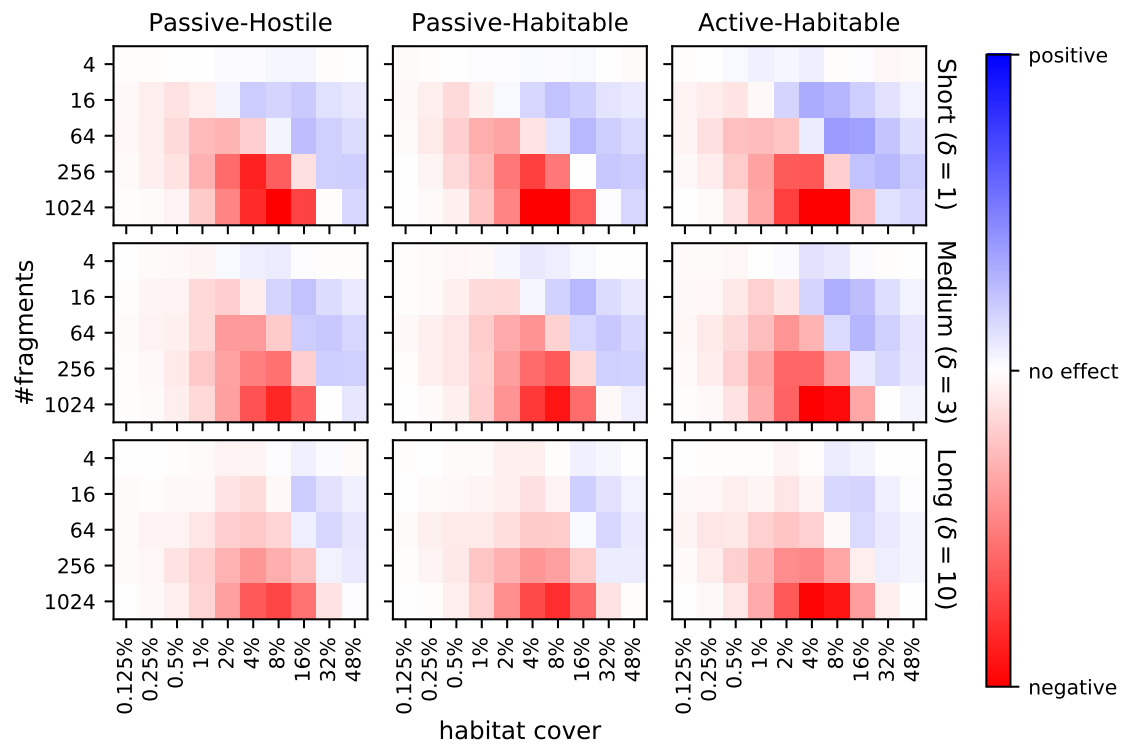


Figure S12: SLOSS analysis on the community of 64 species in a  $100 \times 100$  landscape with an environmental gradient.

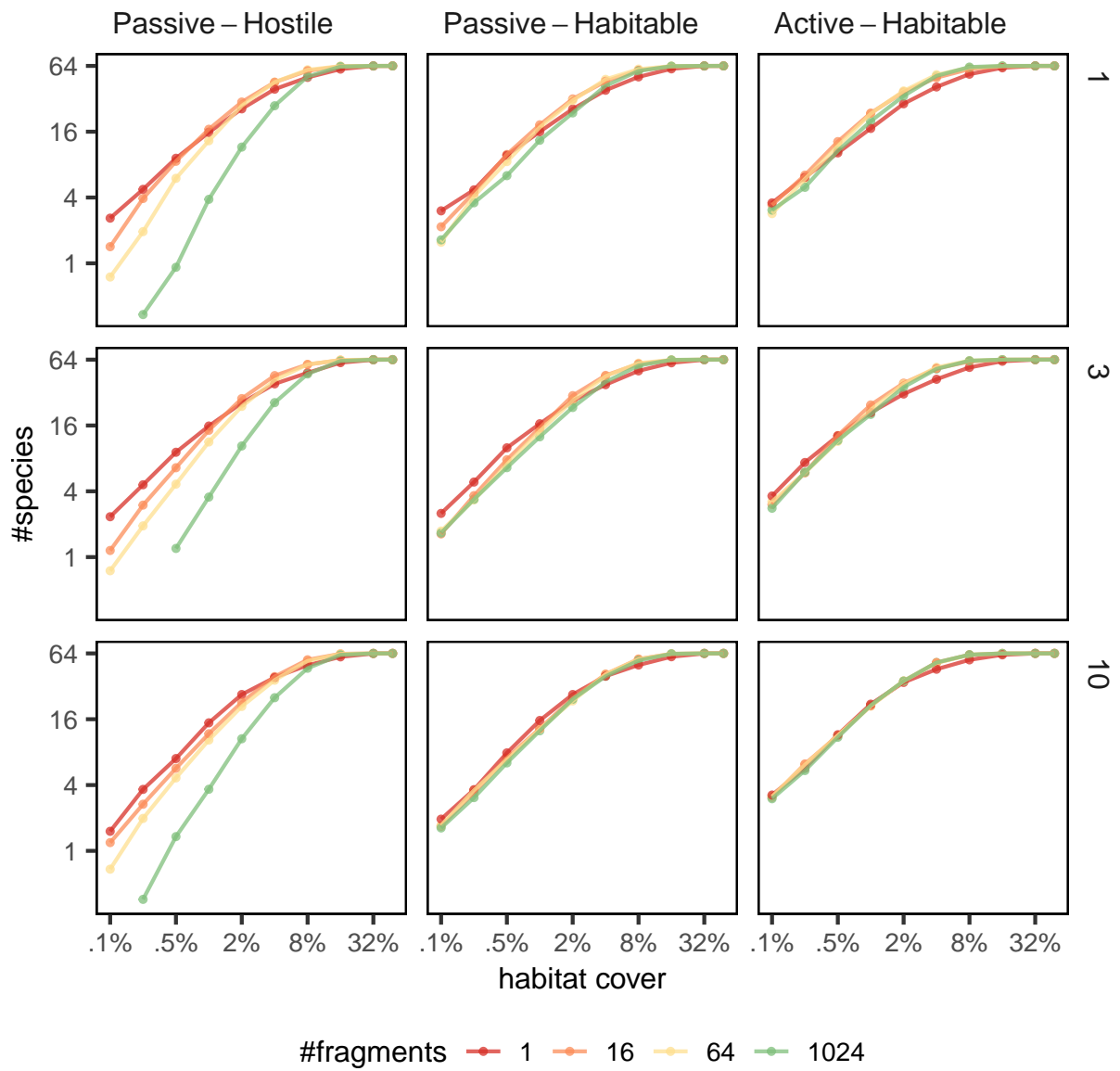


Figure S13: SFAR analysis on the community of 64 species in a  $100 \times 100$  landscape with an environmental gradient.

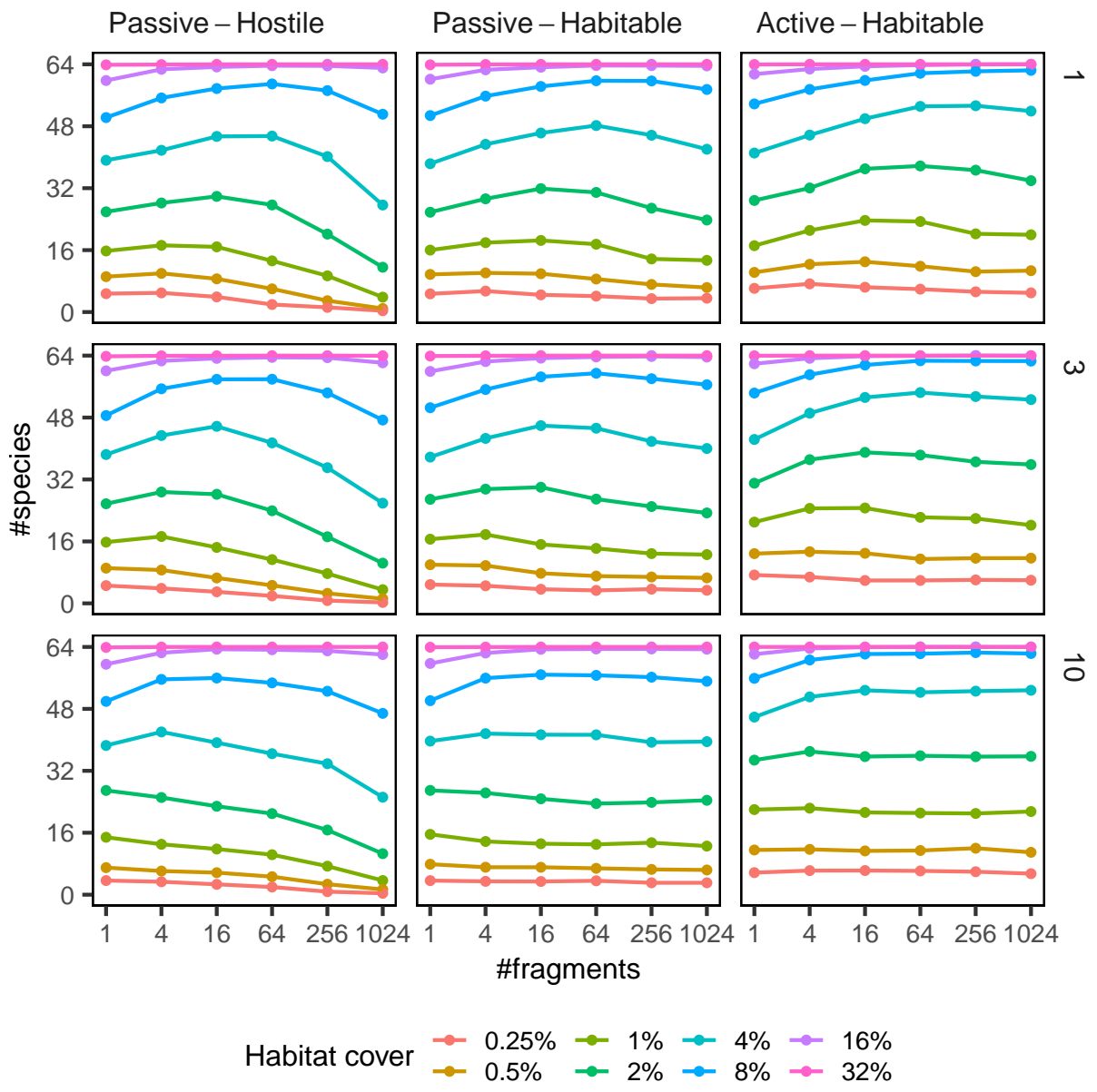


Figure S14: Species richness as a function of habitat fragmentation in a community of 64 species in a  $100 \times 100$  landscape with an environmental gradient.

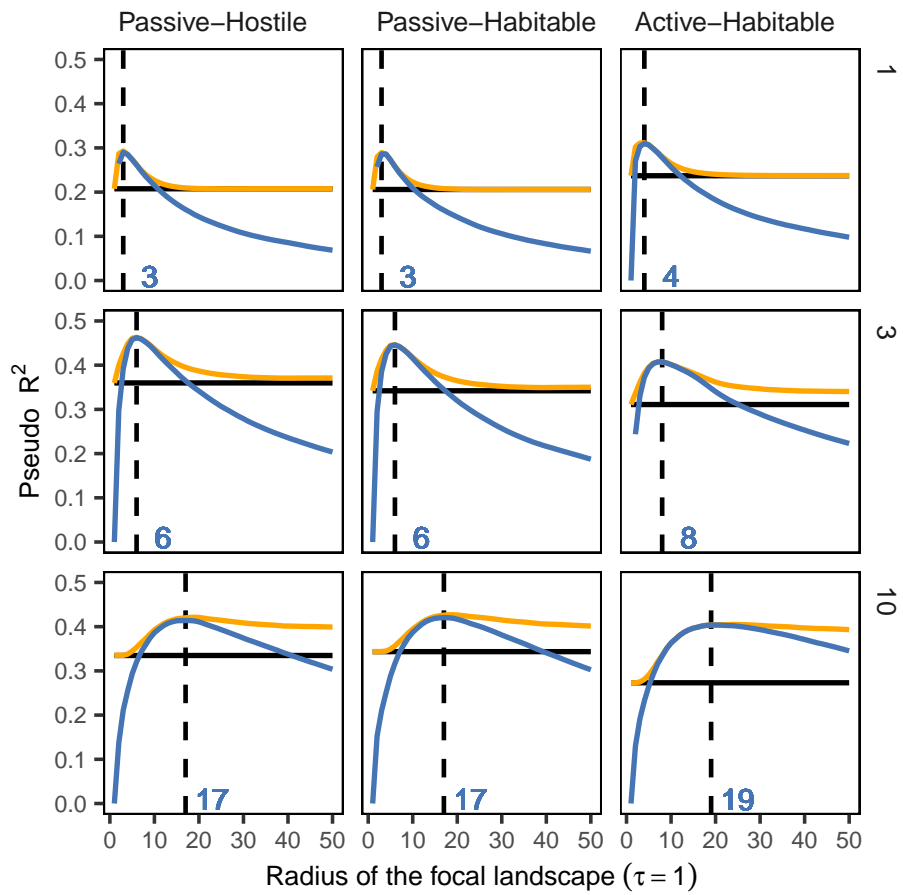


Figure S15: Inferring the appropriate scale of local landscape and testing the sample area effect on a community of size 64 with an environmental gradient. The radius of the sample site is  $\tau = 1$ .



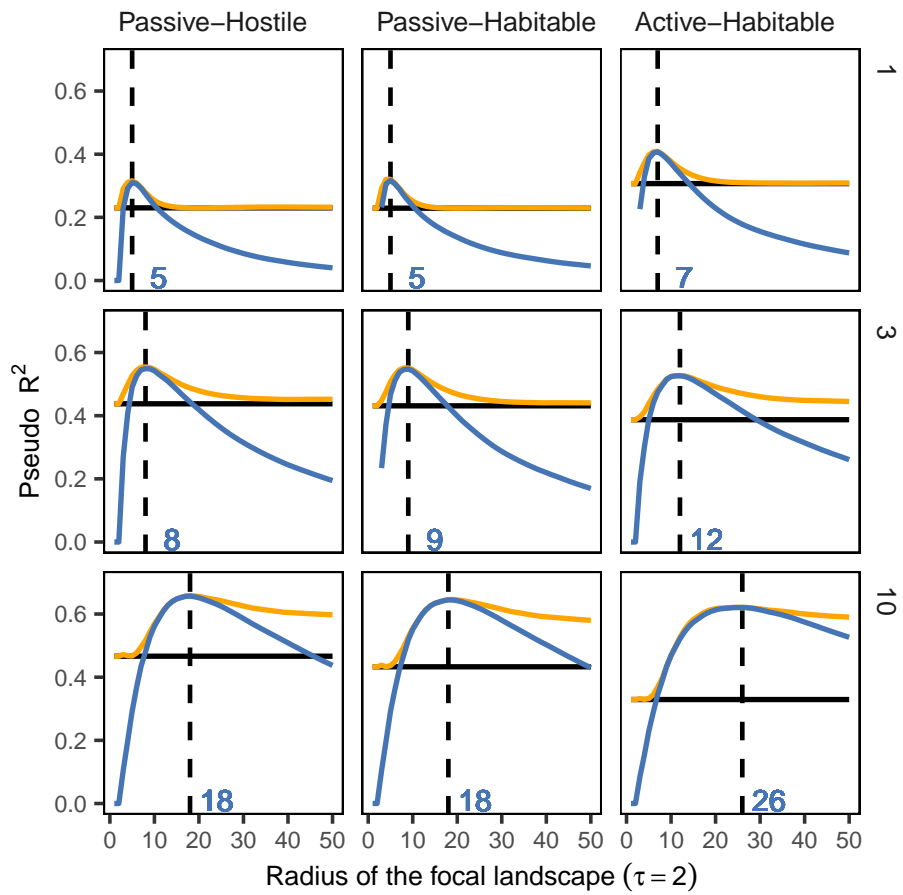


Figure S16: Inferring the appropriate scale of local landscape and testing the sample area effect on a neutral community of size 32. The radius of the sample site is  $\tau = 2$ .

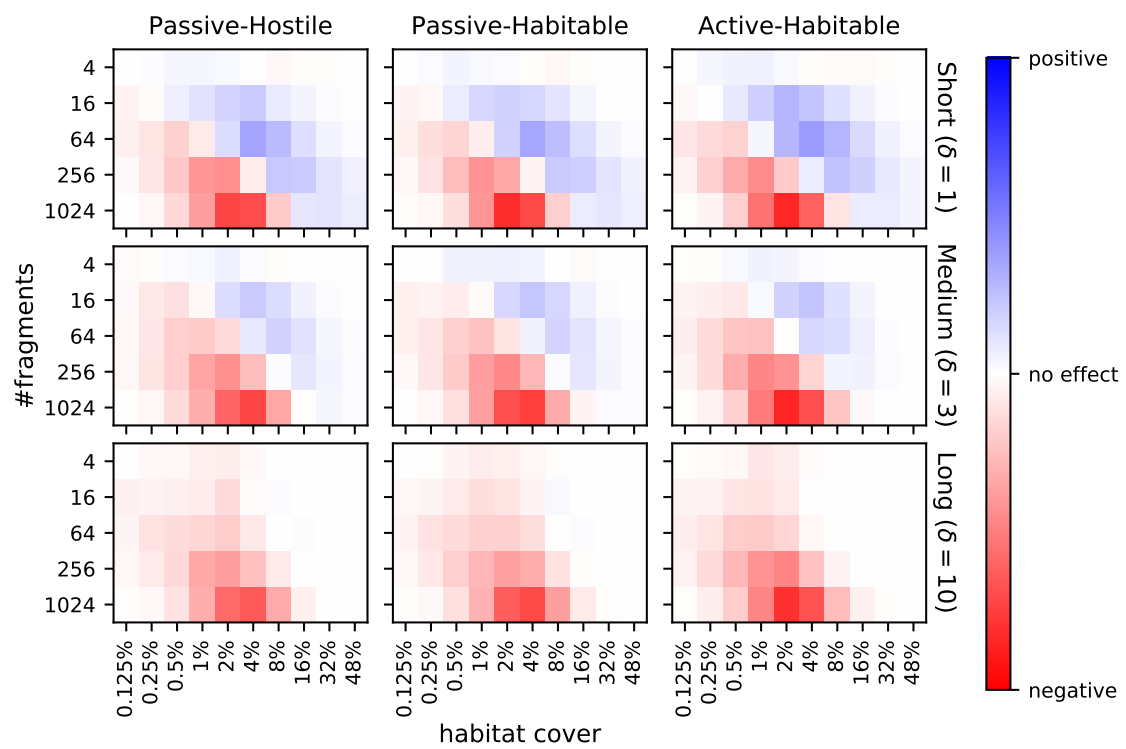


Figure S17: SLOSS analysis of the neutral community of size 32 species in a  $100 \times 100$  landscape.

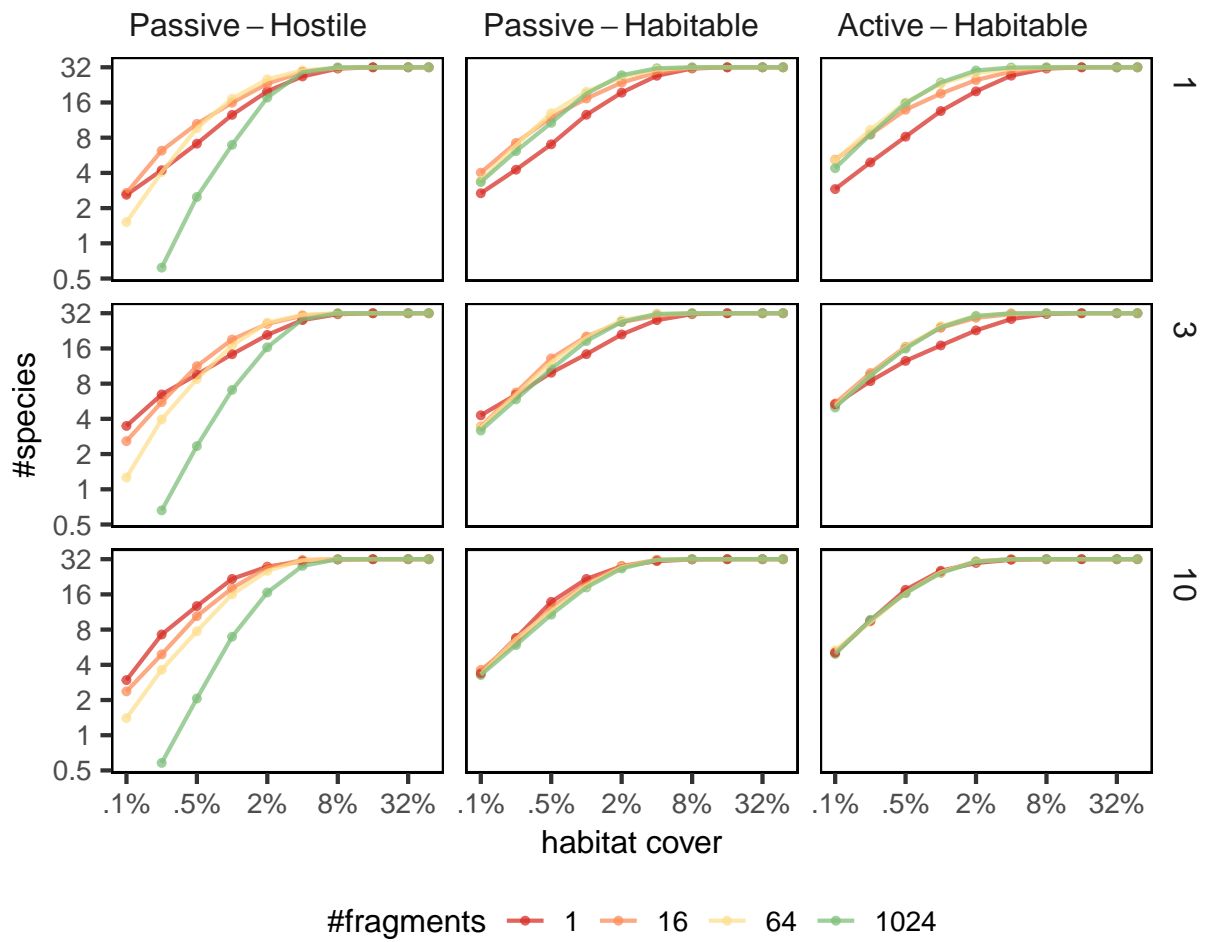


Figure S18: SFAR analysis on the neutral community of size 32 species in a  $100 \times 100$  landscape.

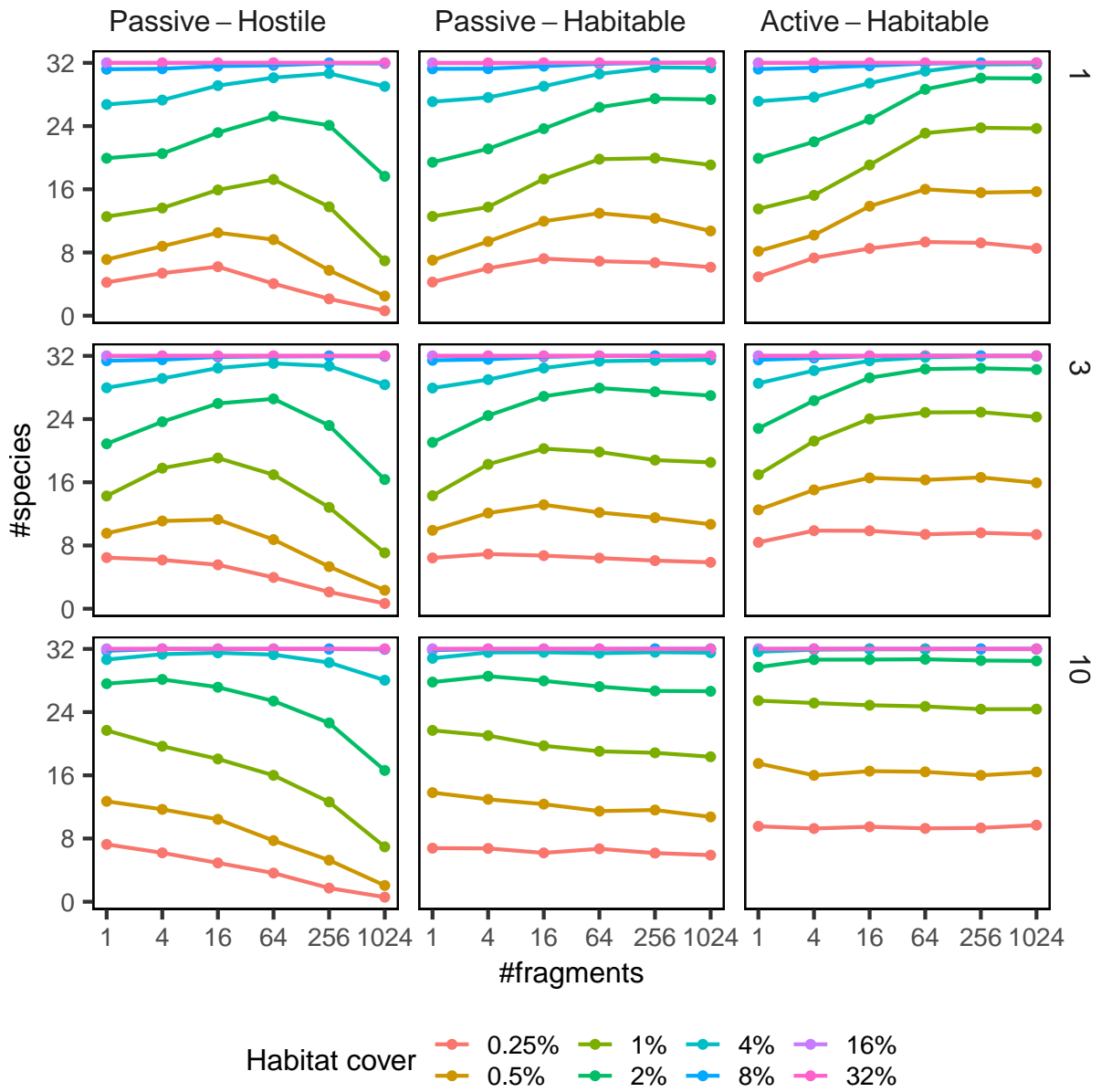


Figure S19: Species richness as a function of habitat fragmentation in a neutral community of 32 species.

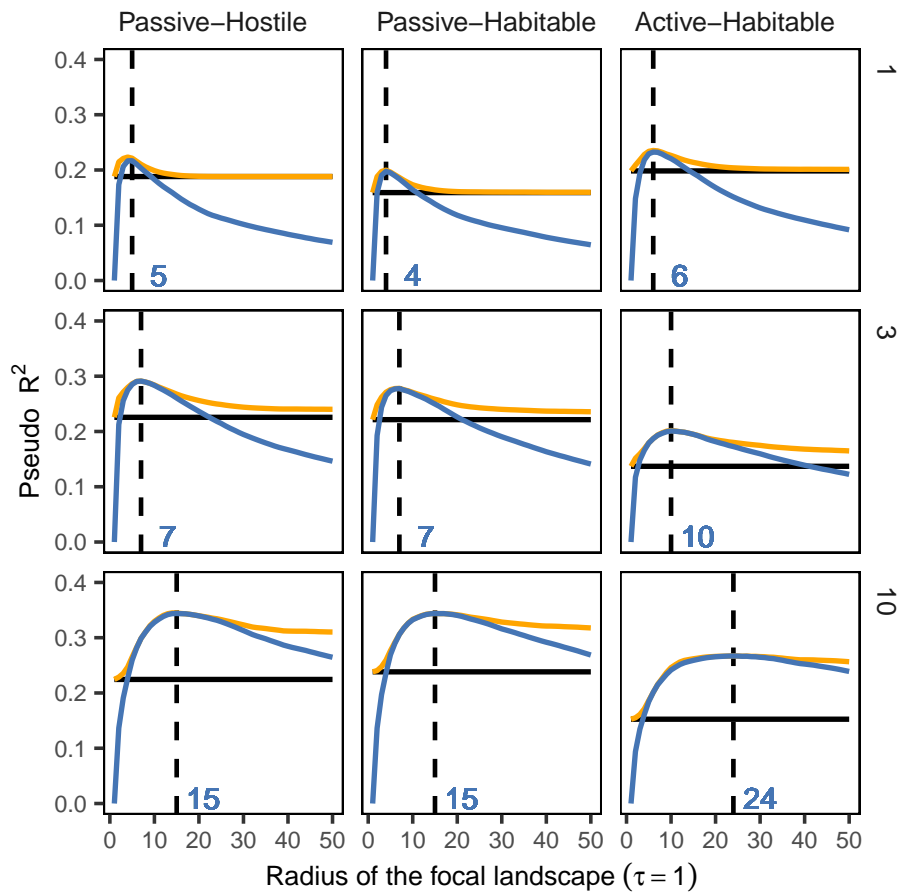


Figure S20: Inferring the appropriate scale of local landscape and testing the sample area effect on a neutral community of size 32. The radius of the sample site is  $\tau = 1$ .

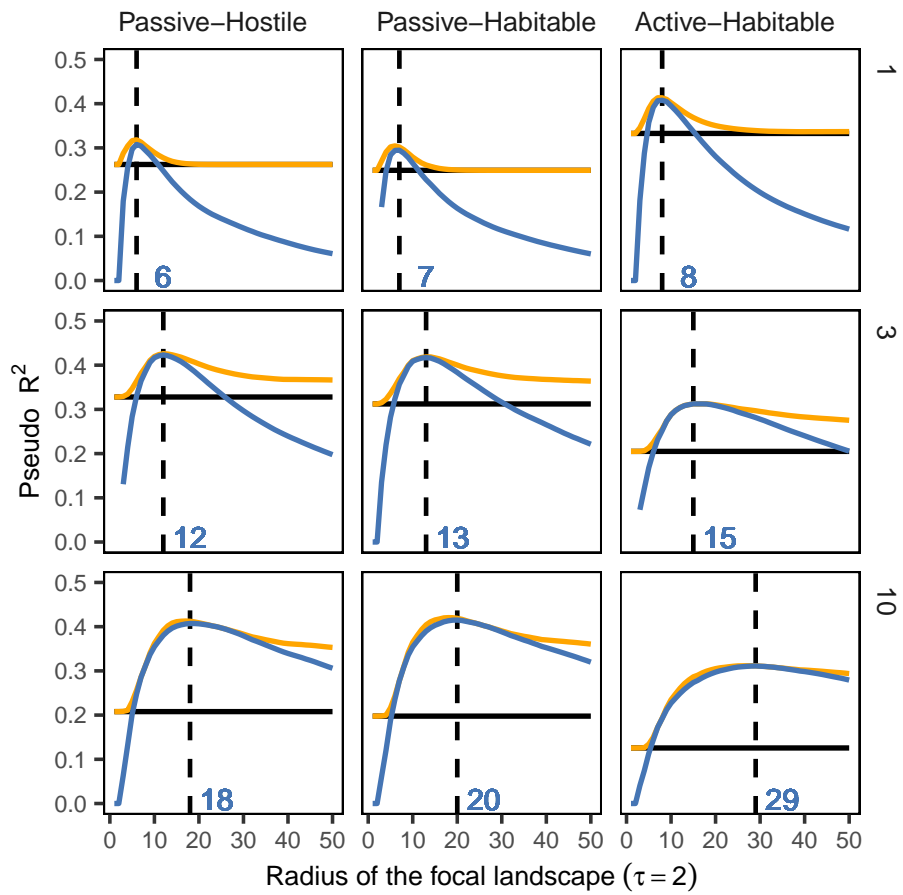


Figure S21: Inferring the appropriate scale of local landscape and testing the sample area effect on a neutral community of size 32. The radius of the sample site is  $\tau = 2$ .

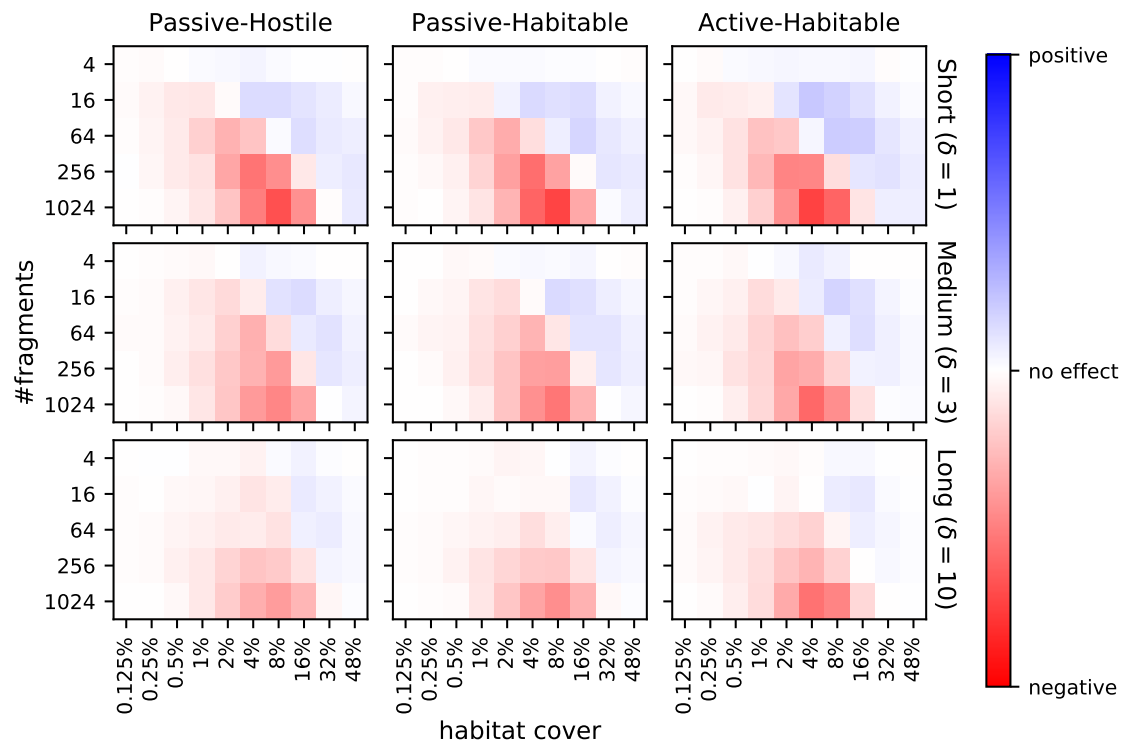


Figure S22: SLOSS analysis of a community of size 32 species in a  $100 \times 100$  landscape with an environmental gradient.

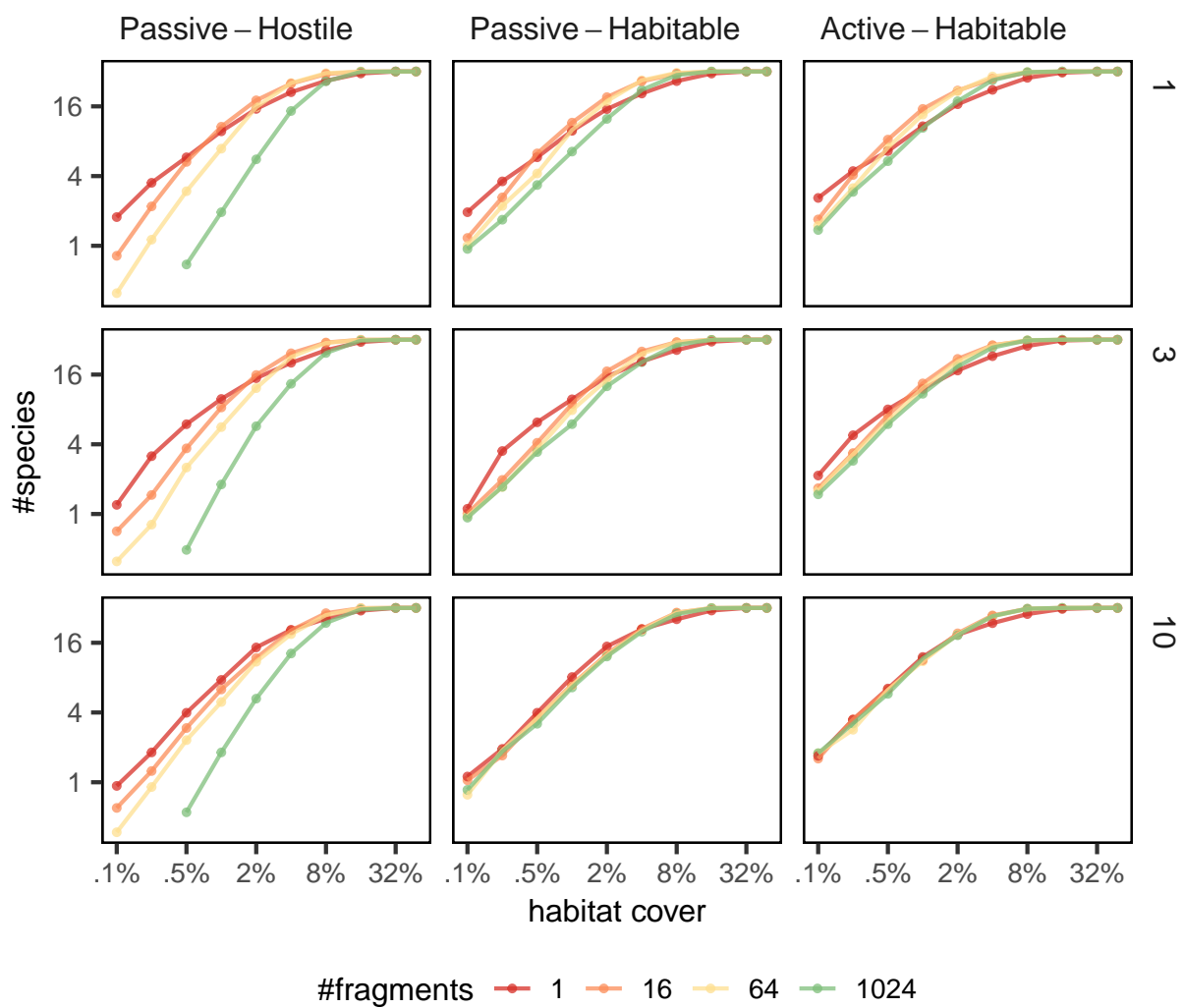


Figure S23: SFAR analysis on the community of size 32 species in a  $100 \times 100$  landscape with an environmental gradient.



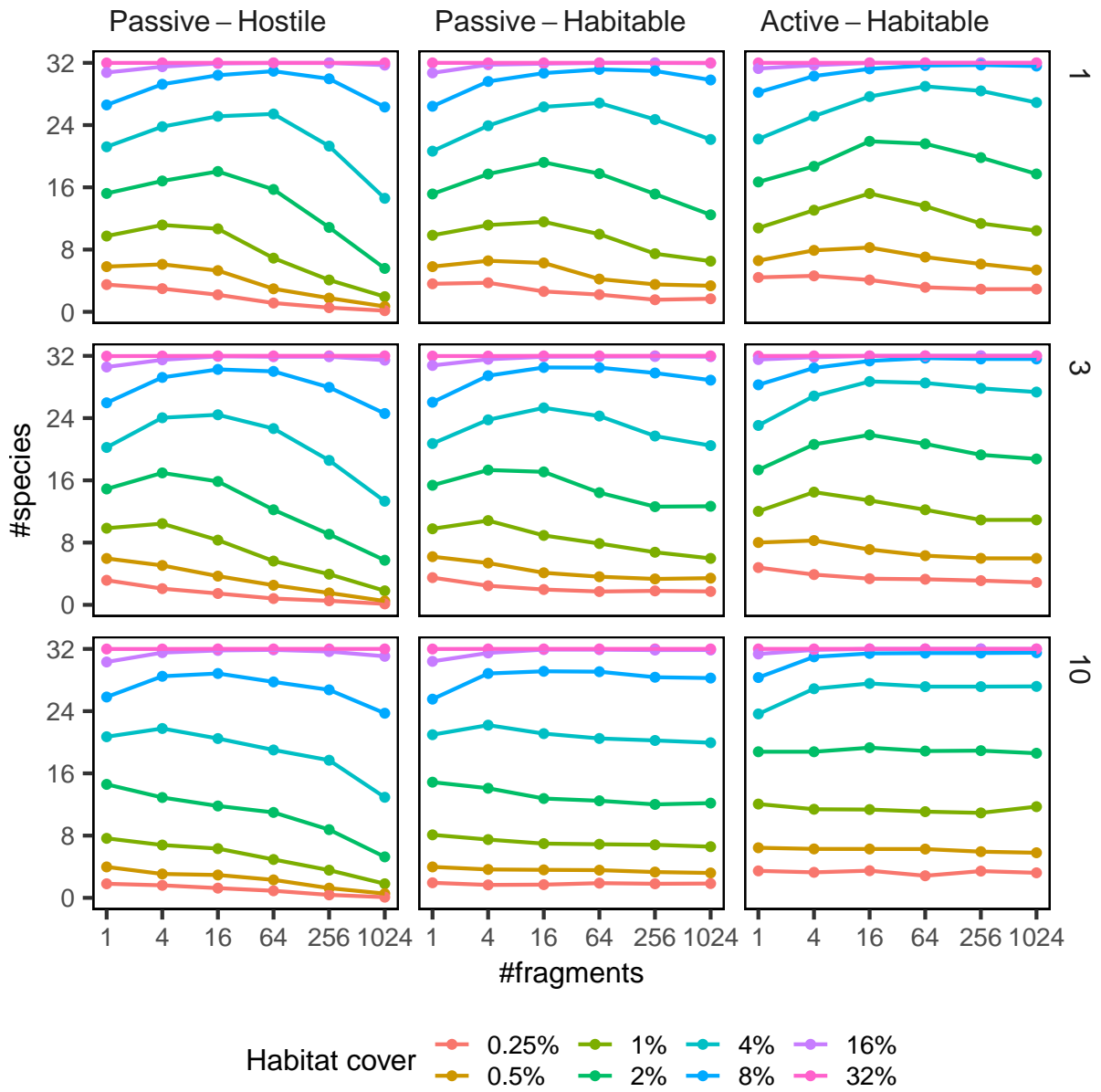


Figure S24: Species richness as a function of habitat fragmentation in a community of 32 species with an environmental gradient.

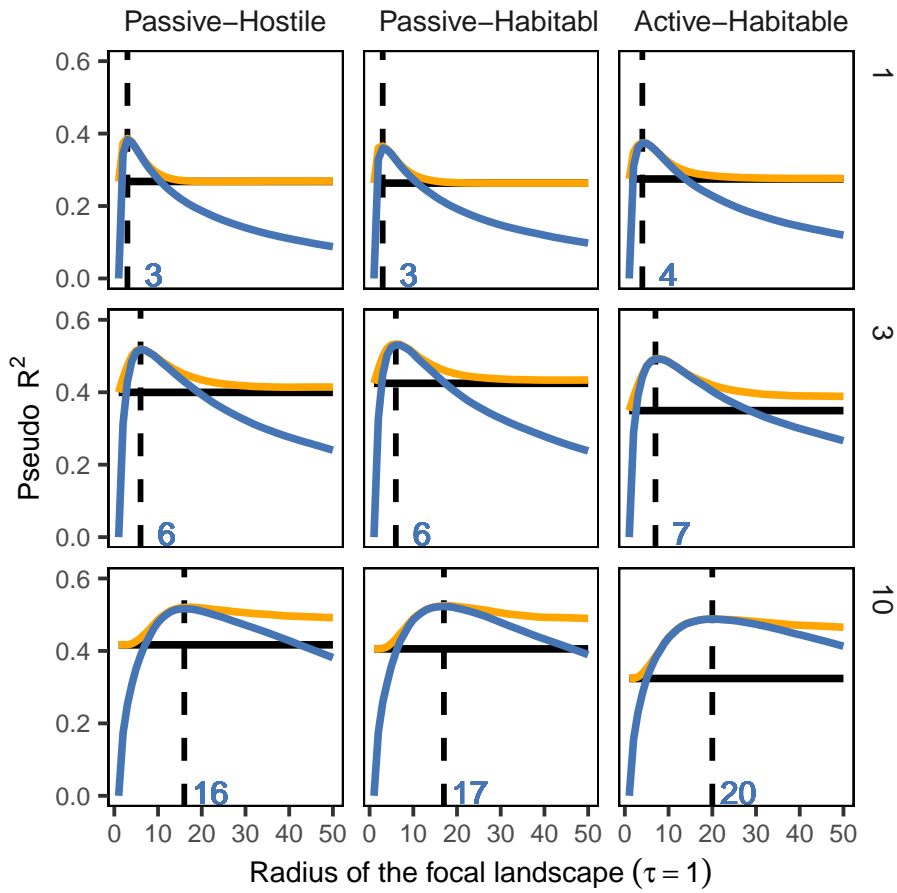


Figure S25: Inferring the appropriate scale of local landscape and testing the sample area effect on a neutral community of size 32. The radius of the sample site is  $\tau = 1$ .

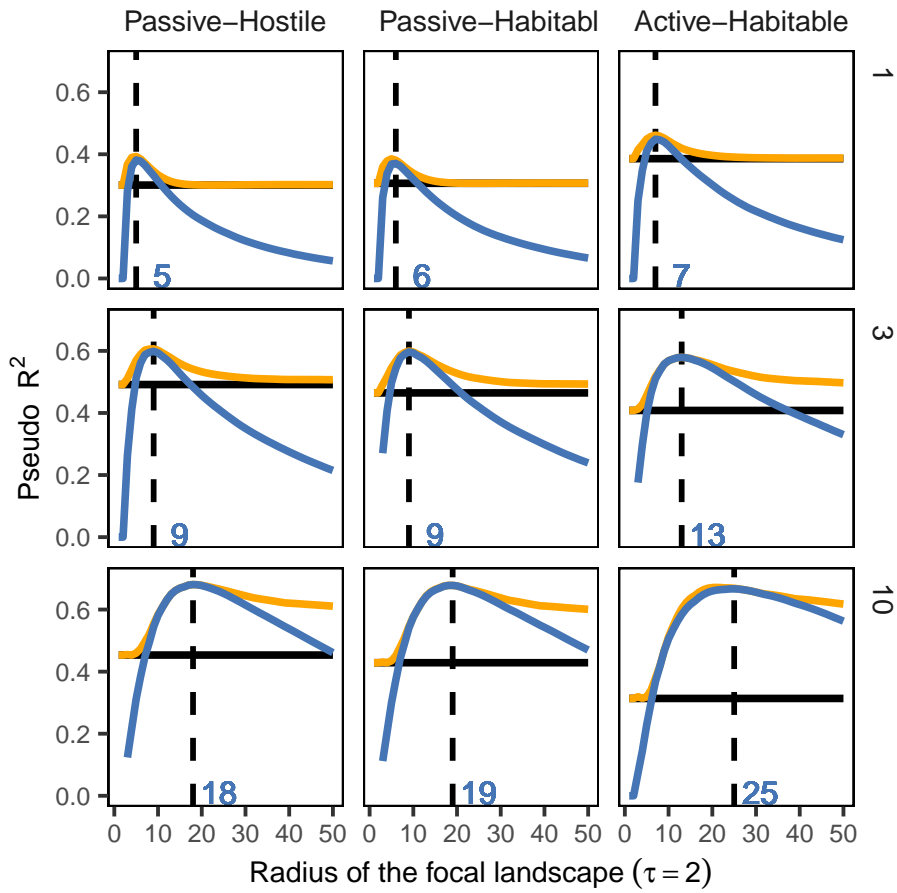


Figure S26: Inferring the appropriate scale of local landscape and testing the sample area effect on a community of size 32. The radius of the sample site is  $\tau = 2$ .

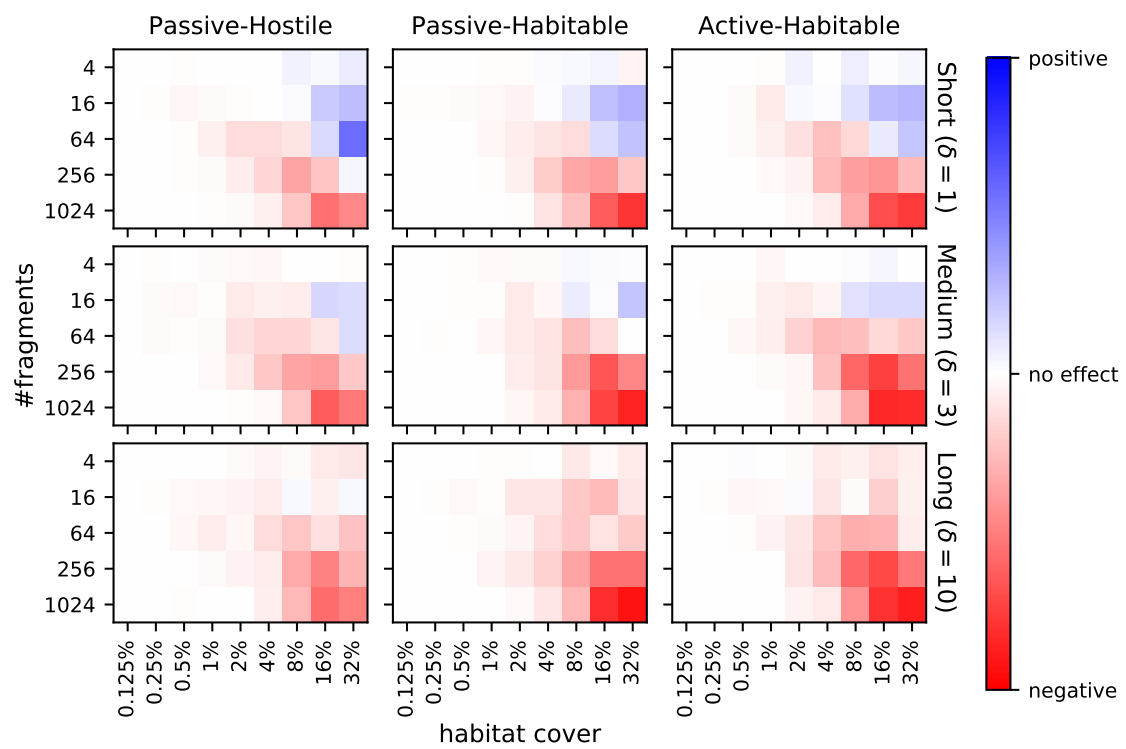


Figure S27: SLOSS analysis of a neutral community of  $S = 64$  species in a  $25 \times 25$  landscape.

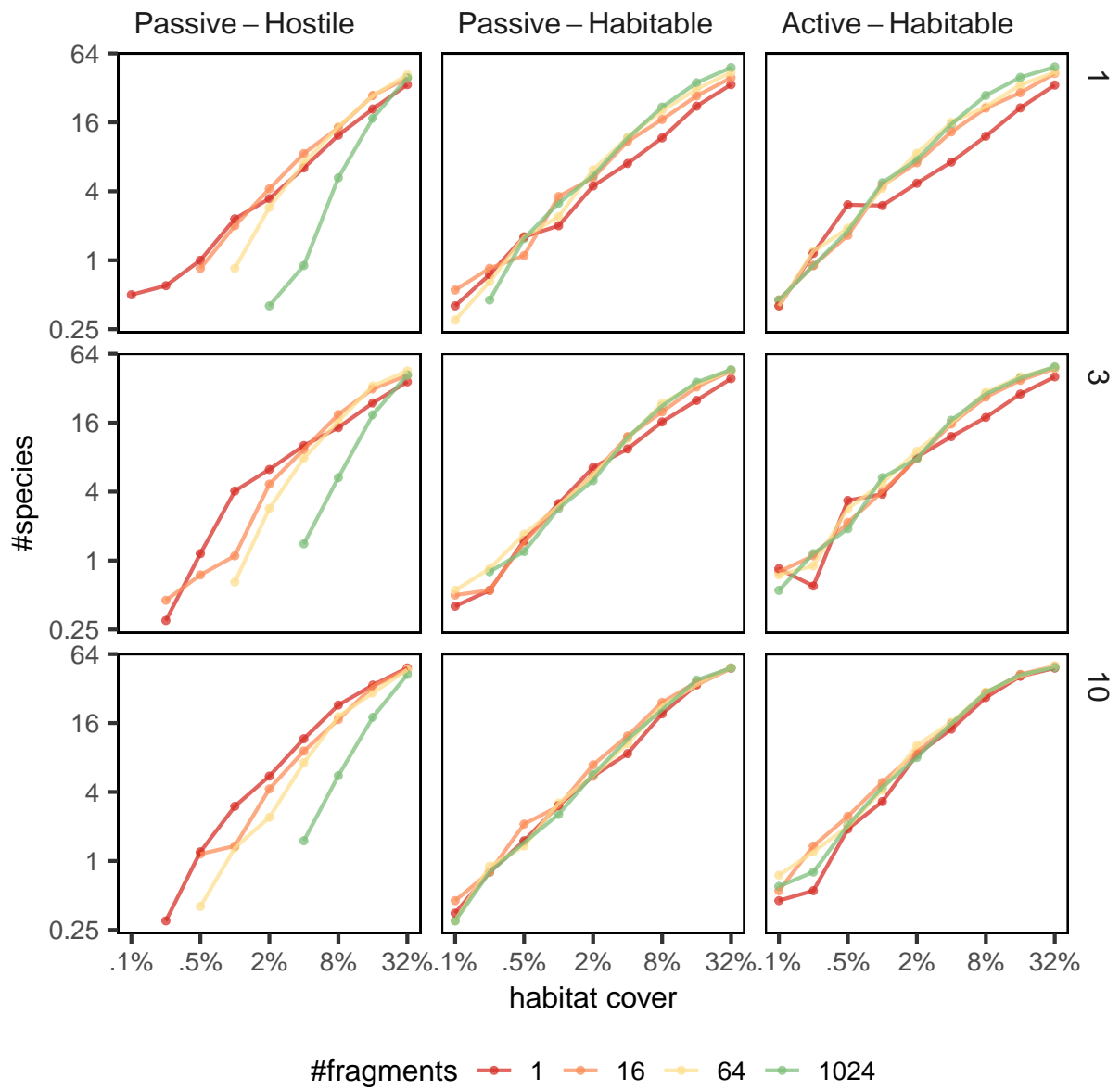


Figure S28: SFAR analysis of of a neutral community of  $S = 64$  species in a  $25 \times 25$  landscape.

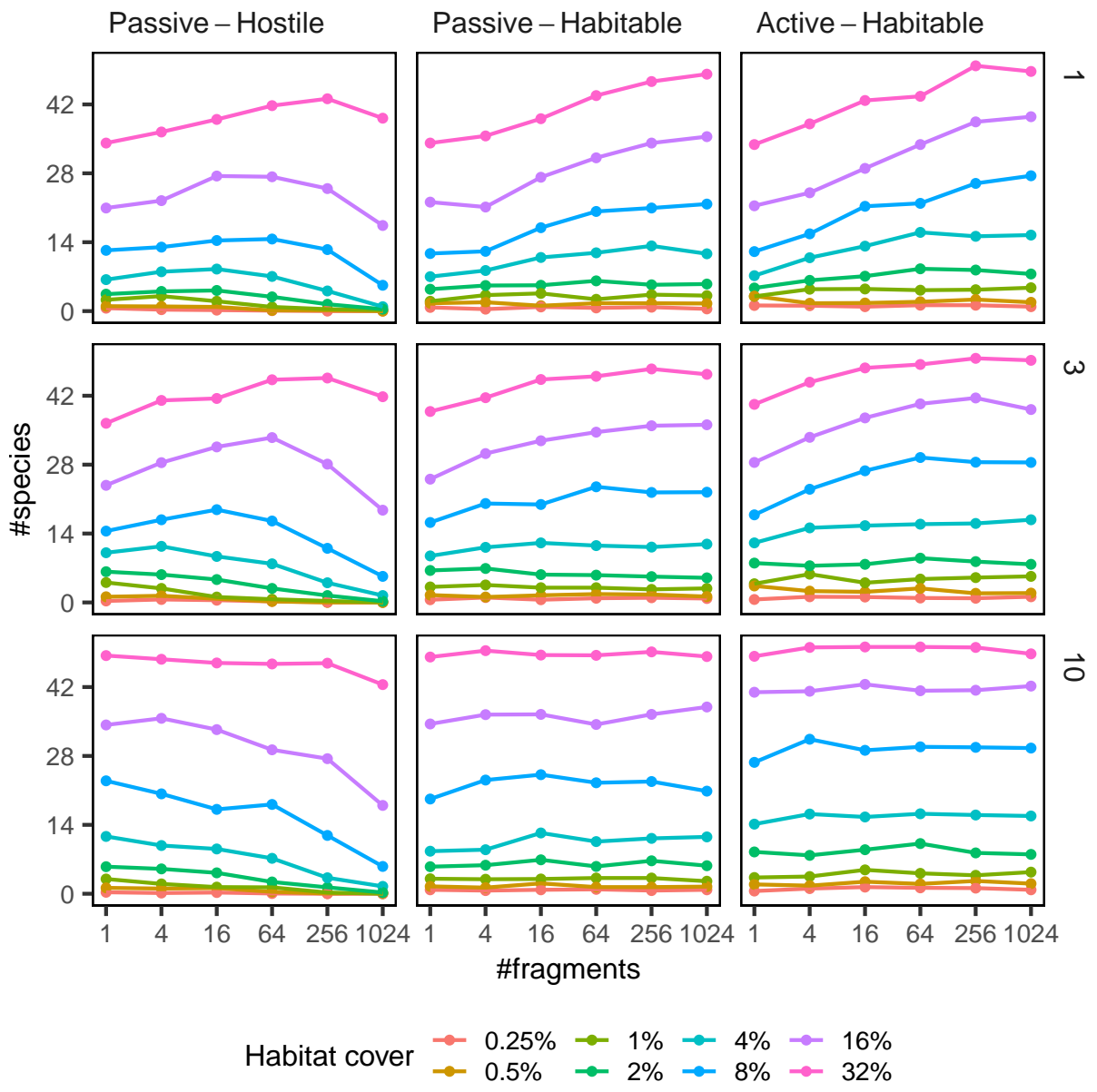


Figure S29: Species richness as a function of habitat fragmentation in a neutral community of  $S = 64$  species in a  $25 \times 25$  landscape.

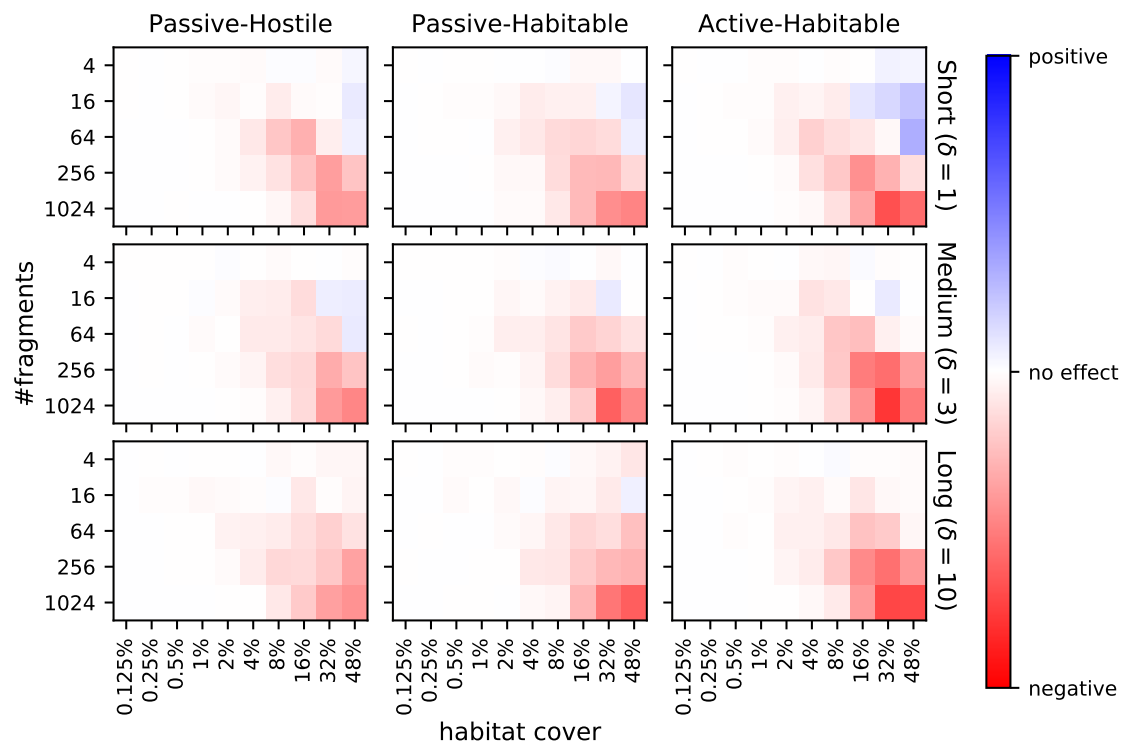


Figure S30: SLOSS analysis of a neutral community of  $S = 64$  species in a  $25 \times 25$  landscape.

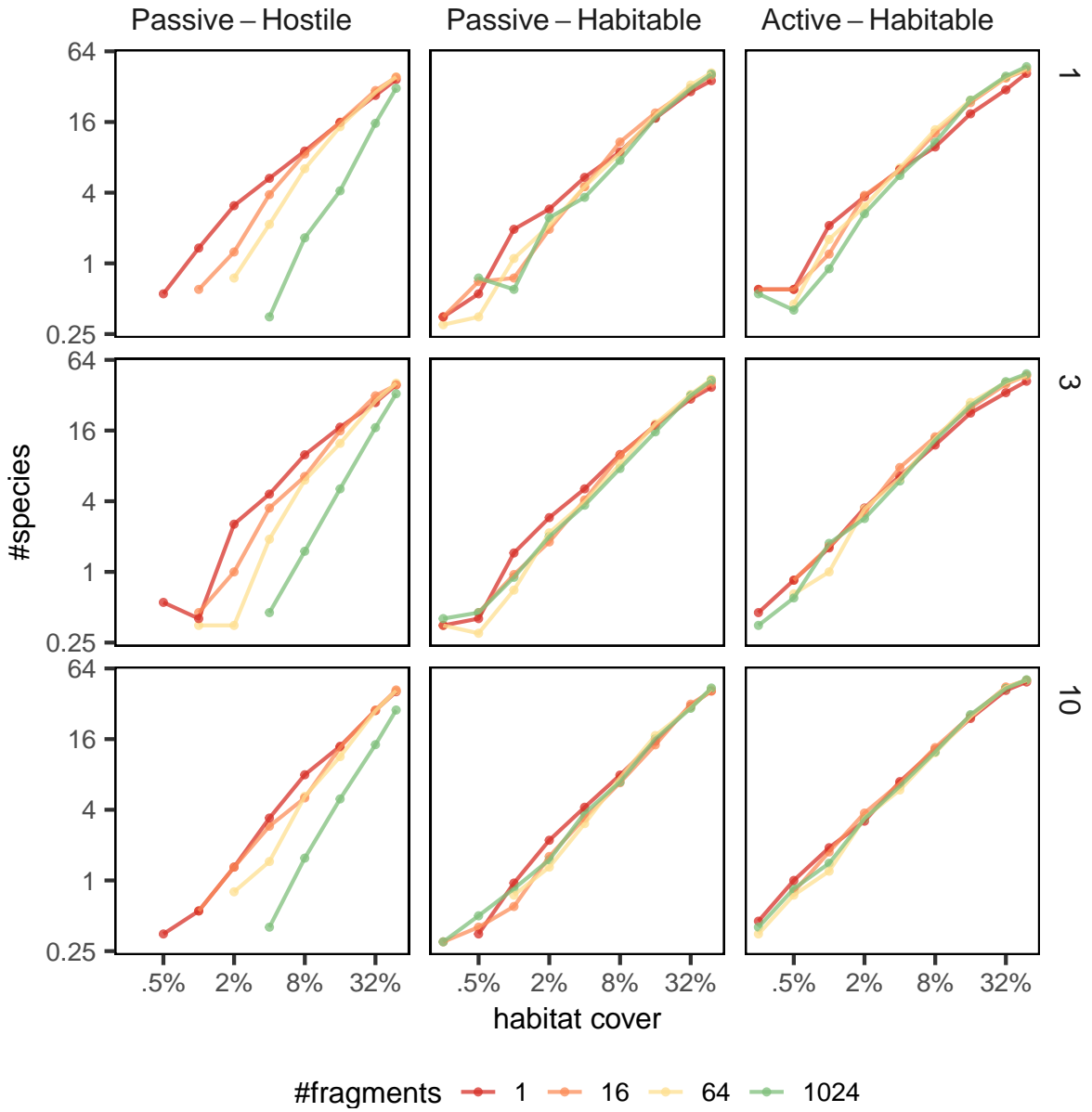


Figure S31: SFAR analysis of of a neutral community of  $S = 64$  species in a  $25 \times 25$  landscape.



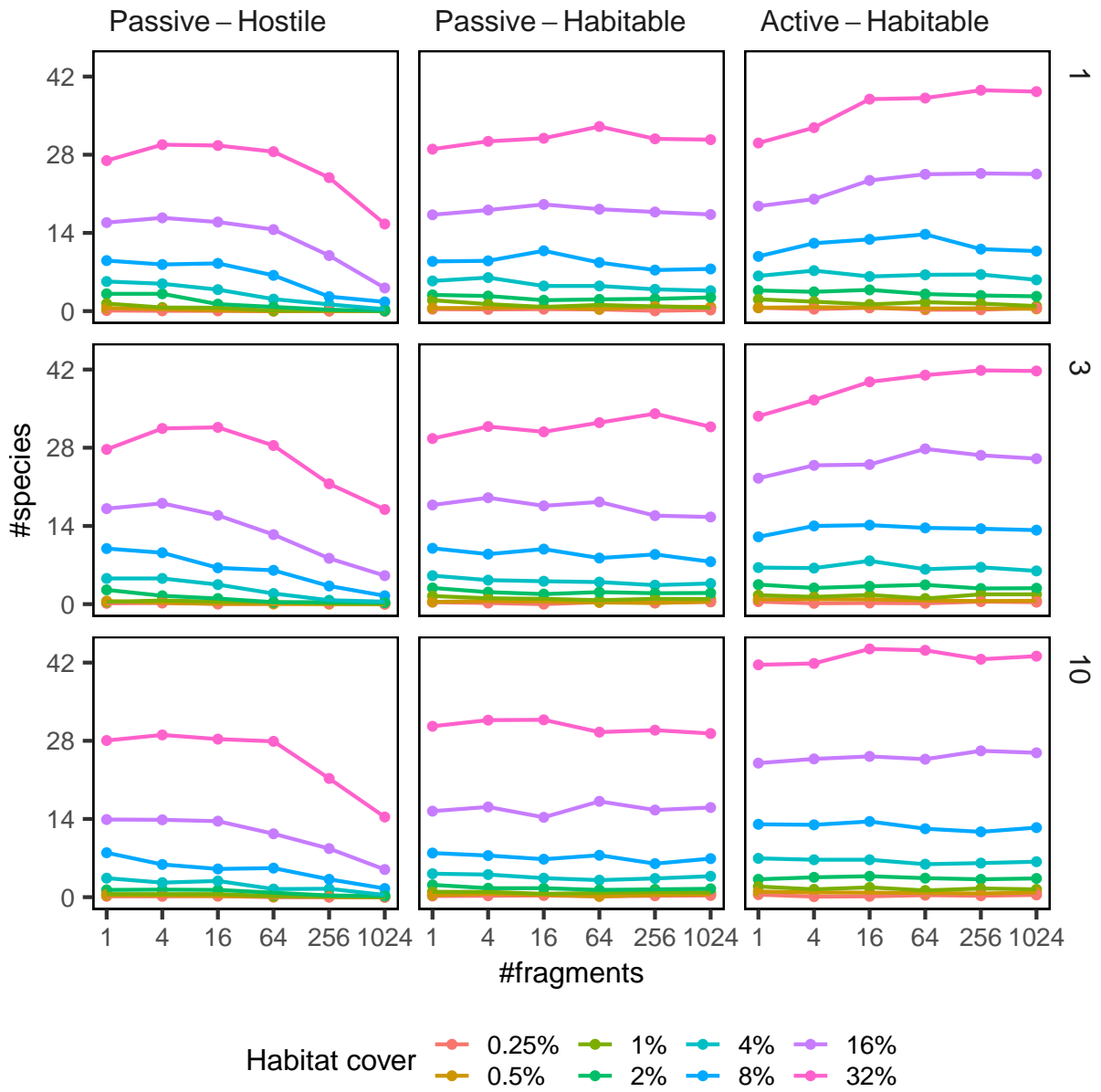


Figure S32: Species richness as a function of habitat fragmentation in a neutral community of  $S = 64$  species in a  $25 \times 25$  landscape.

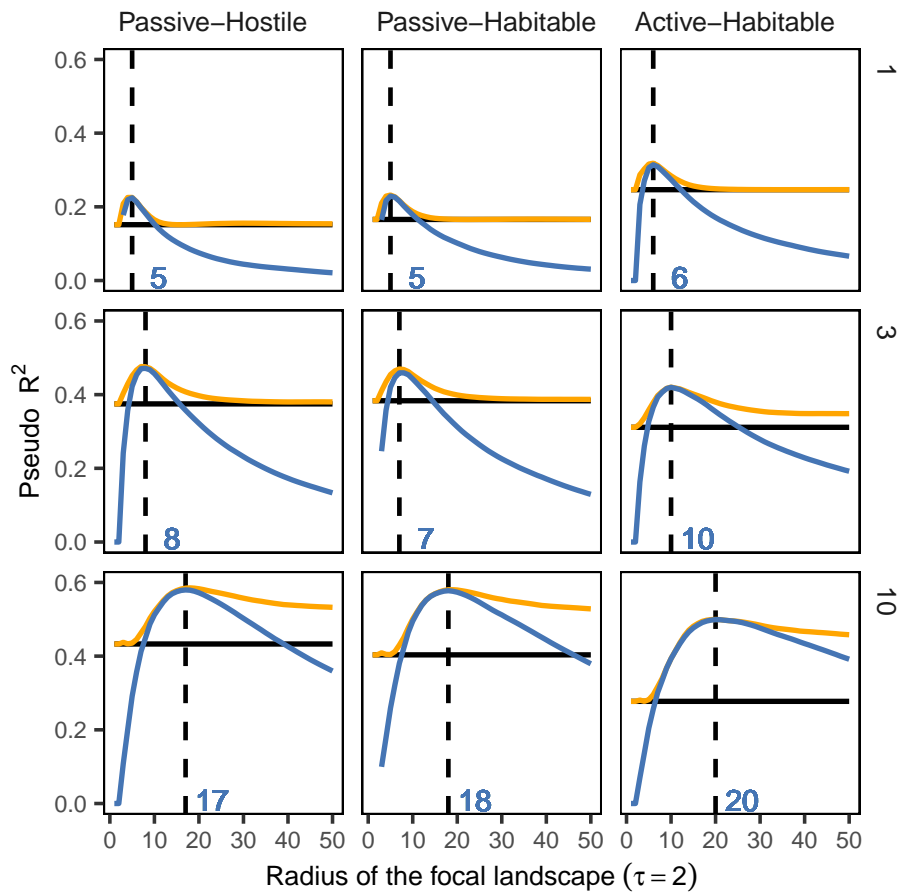


Figure S33: Inferring the appropriate scale of local landscape and testing the sample area effect.

This corresponds to the experiment given in the main text, but the radius of the sample site is  $\tau = 2$ .

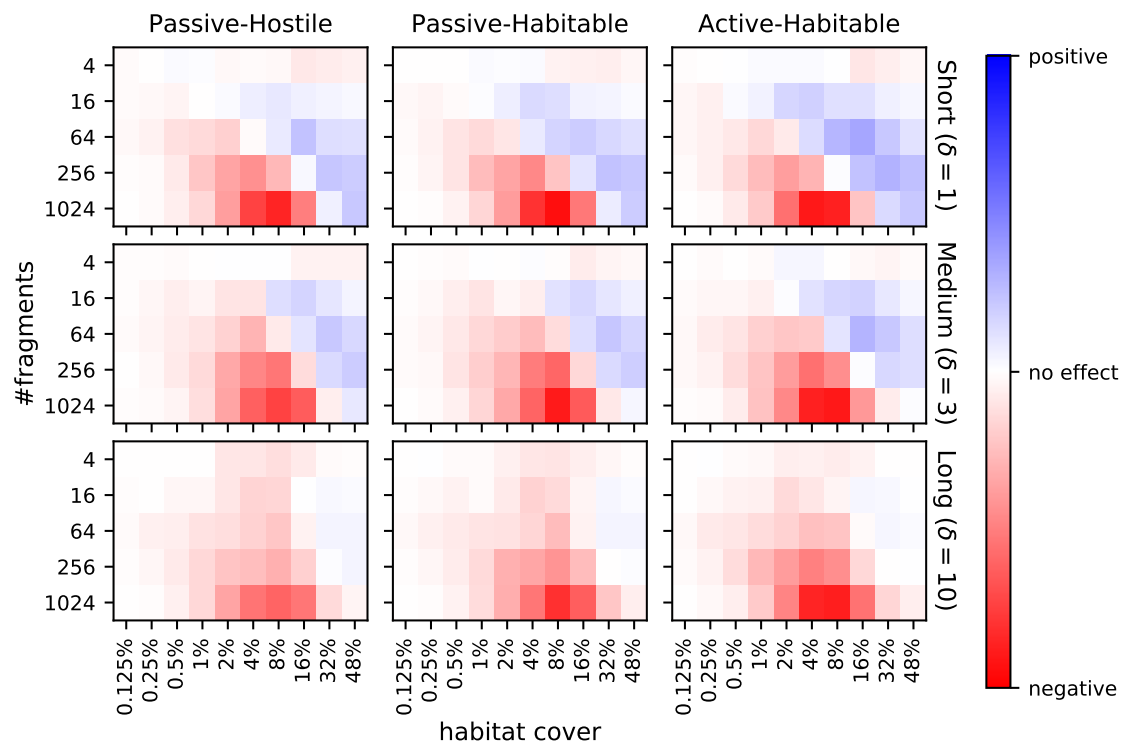


Figure S34: Summary of the SLOSS analysis under the alternative parameterisation (Appendix C.6).

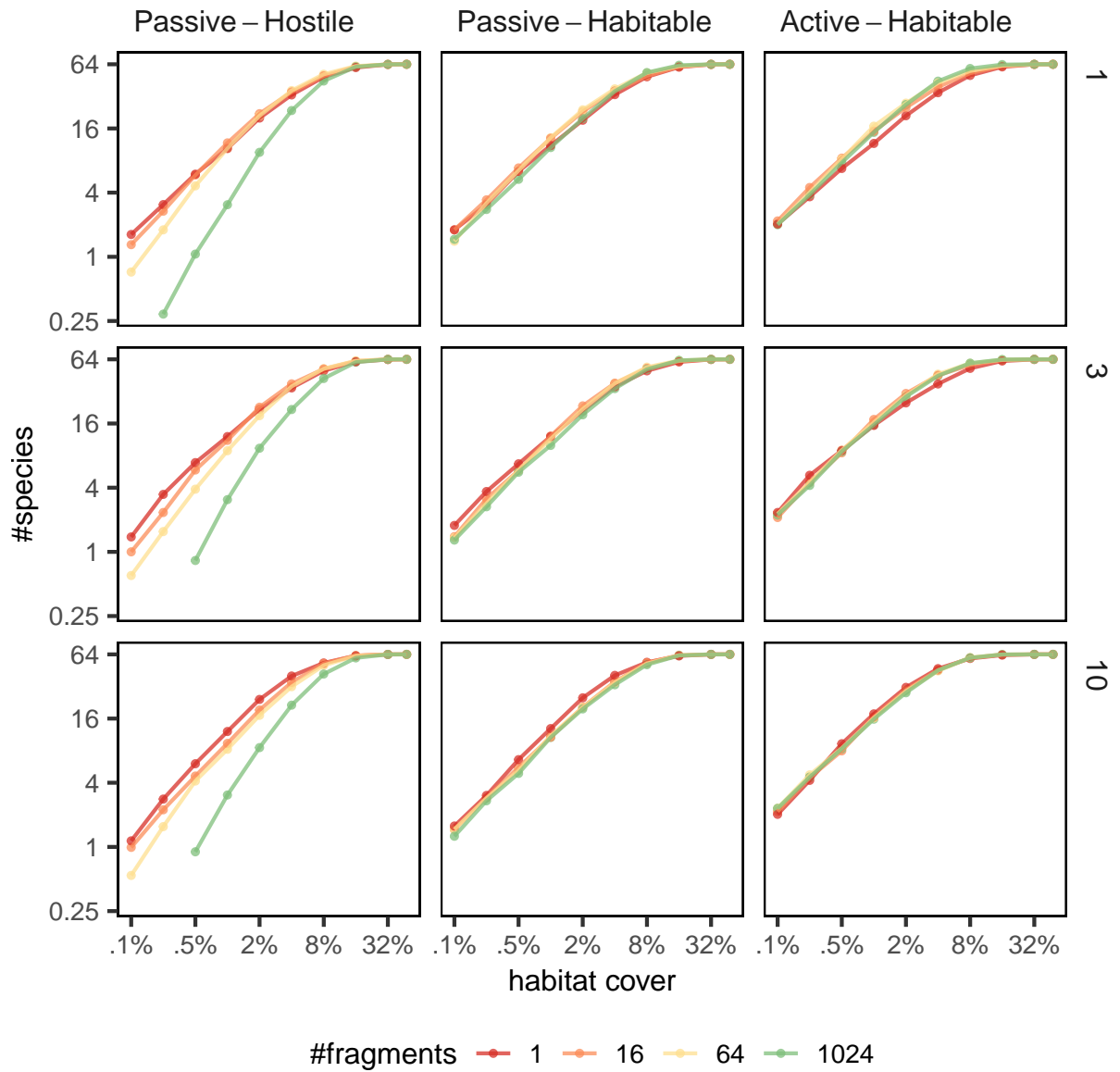


Figure S35: Summary of the SFAR analysis under the alternative parameterisation (Appendix C.6).

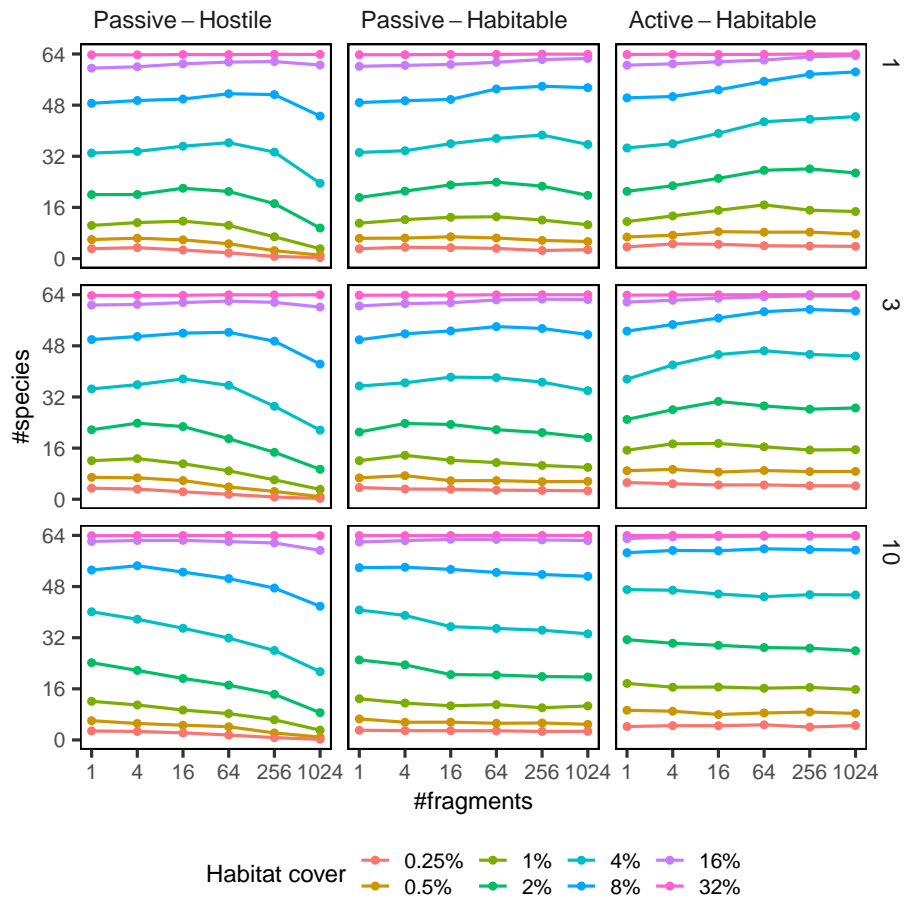


Figure S36: Species richness as a function of habitat fragmentation under the alternative parameterization (Appendix C.6).

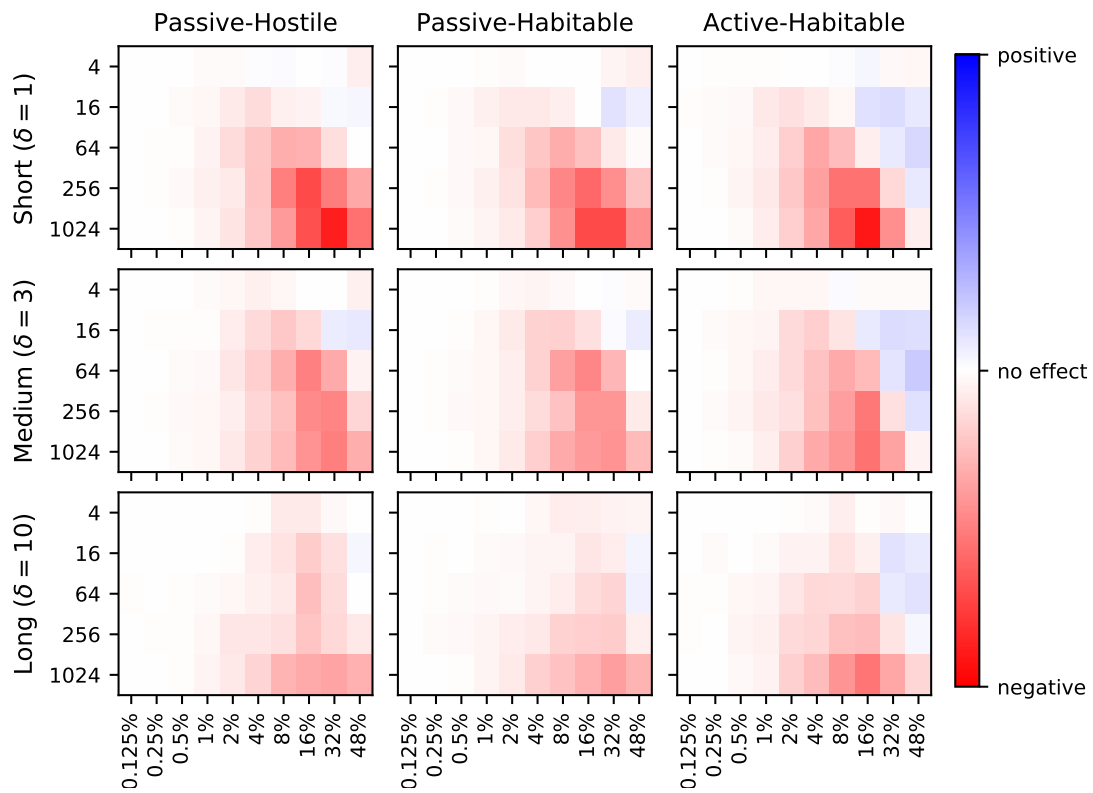


Figure S37: Summary of the SLOSS analysis under the alternative parameterisation (Appendix C.6) in landscapes with environmental gradients (see Fig. 2b in the main text for figure explanation).

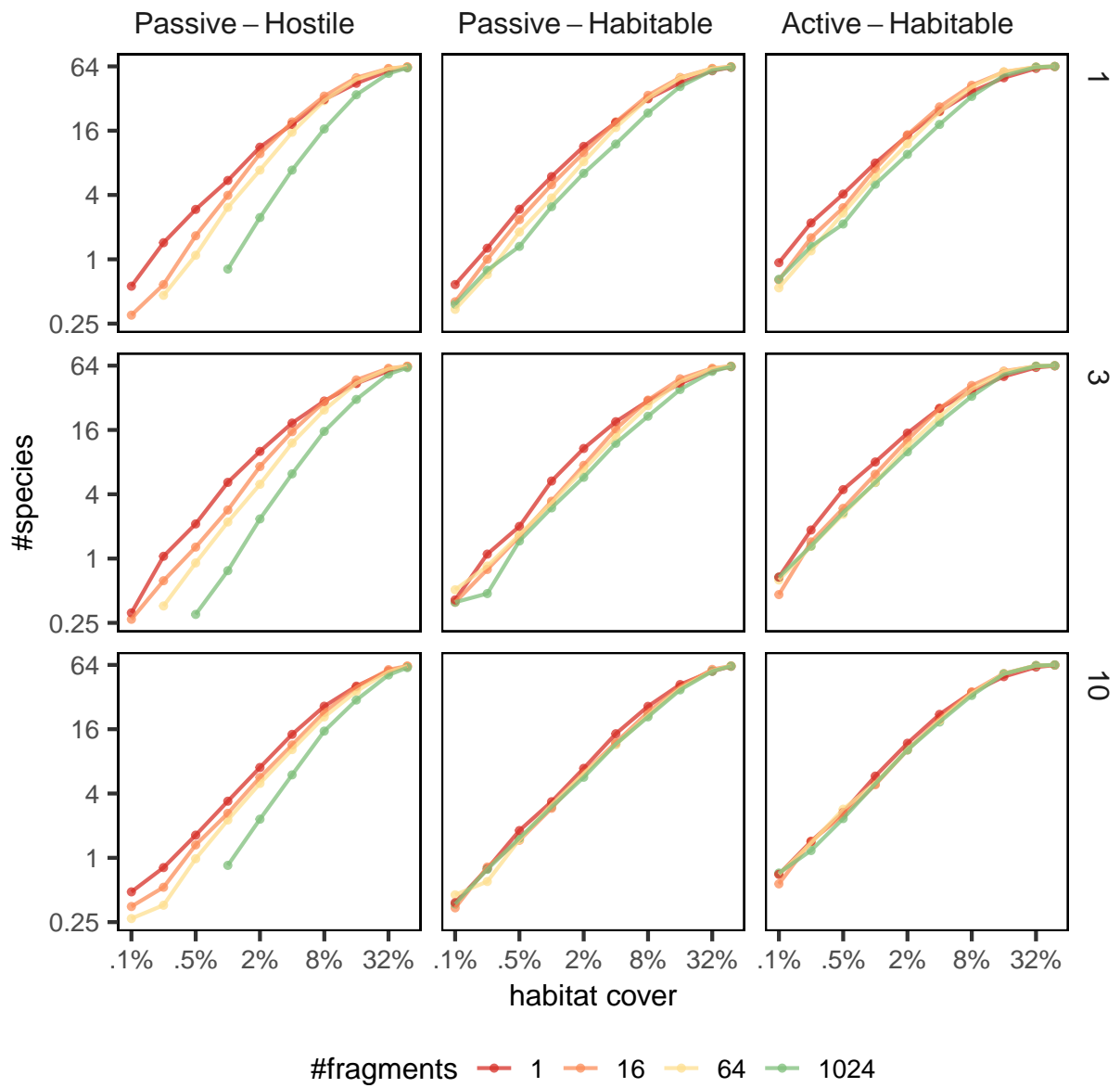


Figure S38: The SFAR analysis under the alternative parameterisation (Appendix C.6) in landscapes with environmental gradients (see Fig. 3 in the main text for figure explanation).

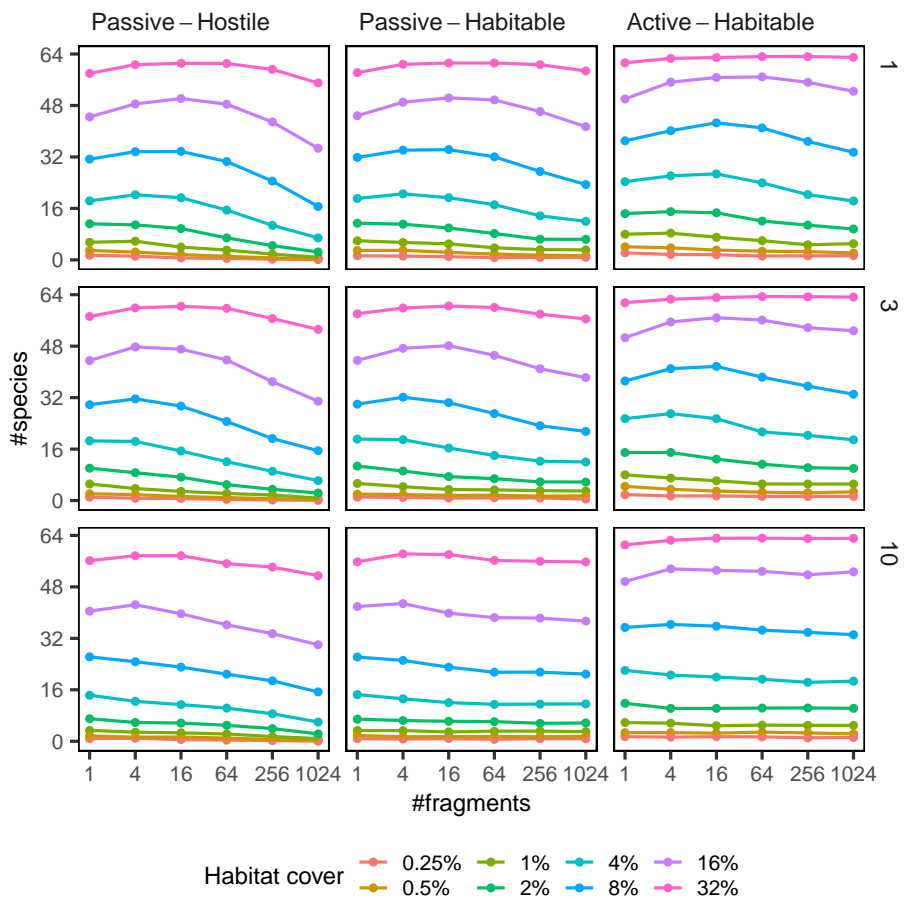


Figure S39: Species richness as a function of habitat fragmentation under the alternative parameterisation (Appendix C.6) in landscapes with environmental gradients (see Fig 4 in the main text for figure explanation).



## 330 **References**

- 331 Ilkka Hanski. *Metapopulation Ecology*. Oxford University Press, 1999.
- 332 M. A. Leibold, M. Holyoak, N. Mouquet, P. Amarasekare, J. M. Chase, M. F. Hoopes, R. D. Holt,  
333 J. B. Shurin, R. Law, D. Tilman, M. Loreau, and A. Gonzalez. The metacommunity concept: A  
334 framework for multi-scale community ecology. *Ecology Letters*, 7(7):601–613, 2004. doi:10.1111/j.  
335 1461-0248.2004.00608.x.
- 336 David Tilman, Robert M. May, Clarence L. Lehman, and Martin A. Nowak. Habitat destruction and  
337 the extinction debt. *Nature*, 371(6492):65–66, 1994. doi:10.1038/371065a0.
- 338 Michel Loreau, Nicolas Mouquet, and Andrew Gonzalez. Biodiversity as spatial insurance in hetero-  
339 geneous landscapes. *Proceedings of the National Academy of Sciences of the United States of America*,  
340 100(22):12765–70, 2003. doi:10.1073/pnas.2235465100.
- 341 Nicolas Mouquet and Michel Loreau. Community patterns in source-sink metacommunities. *The*  
342 *American Naturalist*, 162(5):544–557, 2003. doi:10.1086/378857.
- 343 Omri Allouche and Ronen Kadmon. A general framework for neutral models of community dynamics.  
344 *Ecology Letters*, 12(12):1287–1297, 2009. doi:10.1111/j.1461-0248.2009.01379.x.
- 345 Shaopeng Wang and Michel Loreau. Biodiversity and ecosystem stability across scales in metacom-  
346 munities. *Ecology Letters*, 19(5):510–518, 2016. doi:10.1111/ele.12582.
- 347 Ricard V. Solé, David Alonso, and Joan Saldaña. Habitat fragmentation and biodiversity collapse in  
348 neutral communities. *Ecological Complexity*, 1(1):65 – 75, 2004. ISSN 1476-945X. doi:10.1016/j.  
349 ecocom.2003.12.003.
- 350 Joel Rybicki and Ilkka Hanski. Species-area relationships and extinctions caused by habitat loss and  
351 fragmentation. *Ecology Letters*, 16(SUPPL.1):27–38, 2013. doi:10.1111/ele.12065.
- 352 Miguel G. Matias, Dominique Gravel, François Guilhaumon, Philippe Desjardins-Proulx, Michel  
353 Loreau, Tamara Münkemüller, and Nicolas Mouquet. Estimates of species extinctions from species-  
354 area relationships strongly depend on ecological context. *Ecography*, 37(5):431–442, 2014.  
355 doi:10.1111/j.1600-0587.2013.00448.x.
- 356 Patrick L. Thompson, Bronwyn Rayfield, and Andrew Gonzalez. Robustness of the spatial insurance  
357 effects of biodiversity to habitat loss. *Evolutionary Ecology Research*, 16:445–460, 2014.

358 Bertrand Fournier, Nicolas Mouquet, Mathew A. Leibold, and Dominique Gravel. An integrative  
359 framework of coexistence mechanisms in competitive metacommunities. *Ecography*, (April):1–12,  
360 2016. doi:10.1111/ecog.02137.

361 Patrick L. Thompson, Bronwyn Rayfield, and Andrew Gonzalez. Loss of habitat and connectivity erodes  
362 species diversity, ecosystem functioning, and stability in metacommunity networks. *Ecography*, 40  
363 (1):98–108, 2017. doi:10.1111/ecog.02558.

364 C.A. Klausmeier. Habitat destruction and extinction in competitive and mutualistic metacommunities.  
365 *Ecology Letters*, 4(1):57–63, 2001. doi:10.1046/j.1461-0248.2001.00195.x.

366 Sona Prakash and André M. de Roos. Habitat destruction in mutualistic metacommunities. *Theoretical*  
367 *Population Biology*, 65(2):153–163, 2004. doi:10.1016/J.TPB.2003.10.004.

368 Miguel A. Fortuna and Jordi Bascompte. Habitat loss and the structure of plant-animal mutualistic  
369 networks. *Ecology Letters*, 9(3):281–286, 2006. doi:10.1111/j.1461-0248.2005.00868.x.

370 Pradeep Pillai, Michel Loreau, and Andrew Gonzalez. A patch-dynamic framework for food web  
371 metacommunities. *Theoretical Ecology*, 3(4):223–237, 2010. doi:10.1007/s12080-009-0065-1.

372 Clarence L. Lehman and David Tilman. Biodiversity, stability, and productivity in competitive  
373 communities. *The American Naturalist*, 156(5):534–552, 2000. doi:10.1086/303402.

374 Dominique Gravel, Charles D. Canham, Marilou Beaudet, and Christian Messier. Reconciling niche  
375 and neutrality: the continuum hypothesis. *Ecology Letters*, 9(4):399–409, 2006. doi:10.1111/j.  
376 1461-0248.2006.00884.x.

377 Jürg B. Logue, Nicolas Mouquet, Hannes Peter, and Helmut Hillebrand. Empirical approaches to  
378 metacommunities: a review and comparison with theory. *Trends in Ecology & Evolution*, 26(9):  
379 482–491, 2011. doi:10.1016/J.TREE.2011.04.009.

380 Bart Haegeman and Michel Loreau. General relationships between consumer dispersal, resource  
381 dispersal and metacommunity diversity. *Ecology Letters*, 17(2):175–184, 2014. doi:10.1111/ele.12214.

382 Dominique Gravel, François Massol, and Mathew A. Leibold. Stability and complexity in model  
383 meta-ecosystems. *Nature Communications*, 7(10):12457, 2016. doi:10.1038/ncomms12457.

384 David Tilman, Clarence L. Lehman, and Chengjun Yin. Habitat destruction, dispersal, and de-  
385 terministic extinction in competitive communities. *The American Naturalist*, 149(3):407–435,  
386 1997.

387 Zhichao Xu, Yang Shen, and Jinbao Liao. Patch dynamics of various plant-animal interactions in  
388 fragmented landscapes. *Ecological Modelling*, 368:27–32, 2018. doi:10.1016/J.ECOLMODEL.2017.11.  
389 017.

390 Otso Ovaskainen, Dmitri Finkelshtein, Oleksandr Kutoviy, Stephen Cornell, Benjamin Bolker, and Yuri  
391 Kondratiev. A general mathematical framework for the analysis of spatiotemporal point processes.  
392 *Theoretical Ecology*, 7(1):101–113, 2014. doi:10.1007/s12080-013-0202-8.

393 Stephen P. Hubbell. *The Unified Neutral Theory of Biodiversity and Biogeography*. Princeton University  
394 Press, 2001. ISBN 9780691021287.

395 Michael A Gibson and Jehoshua Bruck. Efficient exact stochastic simulation of chemical systems with  
396 many species and many channels. *The journal of physical chemistry A*, 104(9):1876–1889, 2000.  
397 doi:10.1021/jp993732q.

398 Daniel T Gillespie. A general method for numerically simulating the stochastic time evolution of  
399 coupled chemical reactions. *Journal of computational physics*, 22(4):403–434, 1976. doi:10.1016/  
400 0021-9991(76)90041-3.

401 Stephen J. Cornell, Yevhen F. Suprunenko, Dmitri Finkelshtein, Panu Somervuo, and Otso Ovaskainen.  
402 A unified framework for analysis of individual-based models in ecology and beyond. *Nature*  
403 *Communications*, 10(4716), 2019. doi:10.1038/s41467-019-12172-y.

404 Joel Rybicki, Nerea Abrego, and Otso Ovaskainen. Online supplementary material, 2019. [https :](https://bitbucket.org/jrybicki/habitat-fragmentation-and-species-diversity)  
405 [//bitbucket.org/jrybicki/habitat-fragmentation-and-species-diversity](https://bitbucket.org/jrybicki/habitat-fragmentation-and-species-diversity).